Department of Mechanical and Aerospace Engineering

Assessing the performance of a reservoir-based water source heat pump

Author: Alasdair Cameron Morton

Supervisor: Mr Paul Tuohy

A thesis submitted in partial fulfilment for the requirement of the degree

Master of Science

Sustainable Engineering: Renewable Energy Systems and the Environment

2013

Abstract

Heat pumps are a technology growing in popularity as a means of generating "renewable" heating for buildings on both small domestic and large industrial scales. Although air or ground source systems are more commonly installed in the UK, water source heat pumps (WSHPs) can also offer benefits over conventional heating when implemented correctly and in suitable conditions. Judging whether a particular body of water may be appropriate as a heat source is not straight-forward however, and there is little guidance available in the literature.

The University of St Andrews in Fife is planning to construct an Energy Centre in the nearby town of Guardbridge, sited on the premises of a former paper mill. The site includes a 37,000 m^3 freshwater reservoir which has the potential to be used as the source of a WSHP, notionally contributing towards heating of buildings which will be on site. This project aims to investigate the feasibility of employing the reservoir as the heat source for a WSHP, and the potential performance of a WSHP scheme in operation across a typical year.

Firstly a mathematical model of the reservoir was created using the open-source Freemat programming environment, using a combination of empirical and first principles energy calculations. This was validated by comparison with a similar existing model and actual depth-temperature measurements performed in the reservoir. Components were then added to model the effect of open and closed-loop heat pump schemes operating in the reservoir and empirical relations for heat pump heating capacity and coefficient of performance (COP) were created using manufacturer's data. The modelling results indicate that while an open-loop scheme would be unable to operate for a significant part of the year, and was therefore deemed unsuitable, a closed-loop scheme has the potential to provide significant heating capacity of greater than 1 MW at a water output temperature of 50^oC or 35^oC, with COPs of approximately 4 – 6 across the year. Therefore the project concludes that further investigation is merited into the potential costs and technicalities of installing and integrating a WSHP operating with the reservoir into the wider project at Guardbridge.

Acknowledgements

Table of Contents

List of figures

List of tables

1 Introduction

The need for alternative and efficient means of energy generation are now undeniable, and with the Scottish government having set a target for 50% gross electricity production from renewable sources by 2020 (The Scottish Government, 2012), there is a need for more efficient homes and workplaces in order to accommodate the changing face of energy provision. Heat pumps are one such technology which may in the future play a key role in the provision of cleaner heating provision, provided that the electricity used to operate them can be obtained from renewable sources. With efficiencies often quoted by manufacturers at around 400%, the advantages seem obvious, but careful consideration must be given to the relative advantages of a heat pump over other heating systems. Significantly, heat pumps operate most efficiently when the heat source supplying them (air, ground or water) is warmer. Therefore performance is generally lower in colder weather when the heat is needed most. In order to assess the merits of a heat pump, each case should then be analysed carefully in order to determine the likely performance and heating capacity which can be obtained from a source.

The University of St Andrews is in the early stages of planning the construction of an energy centre, which will employ a number of renewable technologies and energy efficient building design in order to reduce electricity and heating demand. As part of this project, an investigation is to be carried out into the potential to use a large reservoir, formerly used to provide cooling water to the paper mill which previously occupied the site, as a heat source for the operation of a water source heat pump (WSHP). In theory, this may be able to fulfil all or some of the heating demand at the energy centre, supplementing a planned biomass boiler system and solar heating panels.

The aim of this project is to provide an initial feasibility analysis of a WSHP operating with the reservoir as a heat source. This will be achieved through mathematical modelling of the reservoir to obtained expected source temperatures, followed by the development of empirical relations to predict the performance of a number of heat pump sizes and configurations, for a range of operating conditions. The interaction of the heat pump and reservoir will finally be assessed by integrating

the mathematical model and heat pump performance data in order to predict the heating capacity and coefficient of performance (COP) which may be expected from the system.

The report will begin with a literature review giving a background into the general operation of heat pumps, a discussion of various different WSHP systems, and existing schemes operating in the UK and elsewhere, and finally a summary of previous mathematical models to predict the temperature behaviour of a water body. The methodology employed will then be elaborated, including a brief description of the reservoir and the Guardbridge site, the theoretical basis for the reservoir model and of the heat pump performance relations formulated. The results of the modelling will follow, including a brief validation of the reservoir model, a discussion of factors affecting the reservoir temperature, and finally a discussion of the expected heat pump performance of open- and closed-loop heat WSHP schemes. It will conclude with a summary of the key findings and suggestions for further work recommended to be performed.

2 Literature review

An initial literature review was conducted in order to investigate a number of topics relating to heat pump operation, surface water GSHPs and reservoir temperature modelling. Firstly, the basic operating principles of heat pumps are described and how performance is measured is discussed. The review then focuses on surface water GSHP systems and their operation, including closed- and open-loop systems, a comparison of the two, and includes a number of examples of lake-based systems currently in operation. The review concludes with a description of three approaches to reservoir temperature modelling which have been previously undertaken.

2.1   Heat Pumps

Heat pumps have seen increasing popularity in the UK, although overall implementation remains relatively low. Total annual installation figures increased from 2,000 in 2006 to 21,000 in 2011 (PostNote, 2013). In 2011, total UK sales were at 366,000, and forecasts predict a total number of installations in 2015 of around 640,000 (Karpathy, 2012). Whether this figure is achieved or not will depend significantly on changes to governmental legislation, particularly the Renewable Heat Premium Payment Scheme (RHPPS) and the Renewable Heat Incentive (RHI).

2.1.1   Basic principles

Heat pumps are used to transfer low-grade heat from a low-temperature source to a body at a higher temperature. This process is commonly used in the household refrigerator, in which heat is extracted from the cold body inside the fridge and released to the external environment (i.e. the kitchen). In the case of a heat pump in a cold climate, the user is generally interested not in the extraction of heat to maintain a cold environment, but in the addition of heat into an already warm environment.

The Clausius statement of the second law of thermodynamics states that a cyclic device cannot be used to transfer heat from a colder to a hotter body without the addition of some work. Therefore, the operation of a heat pump requires electrical energy. The basic operation of a heat pump relies on the vapour-compression cycle. An example of the simplest case is shown in Figure 2.1 below and is known as the reversed Carnot cycle.
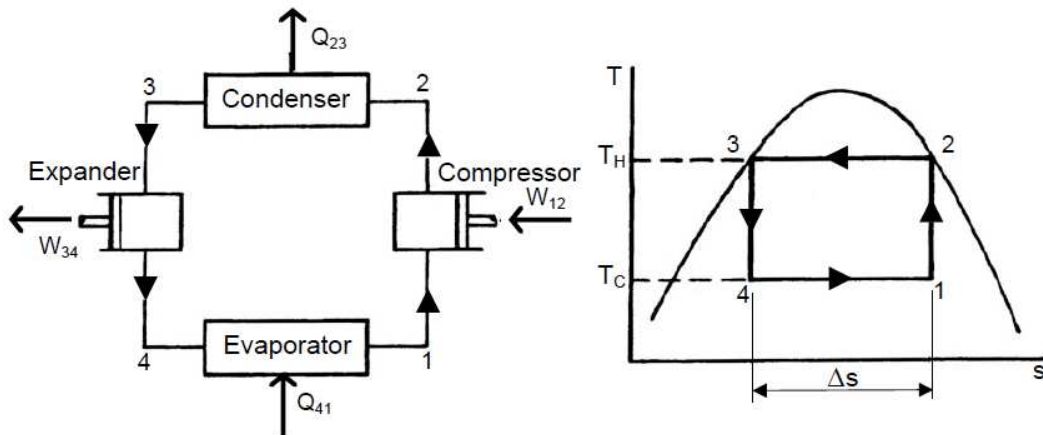
Figure 2.1: Reversed Carnot cycle (Tuohy, 2013)

A working fluid, also known as a refrigerant, is used to transfer heat from one body to another. Looking first at point 1, the refrigerant exists as a liquid-vapour mixture. A compressor is used to increase the temperature and pressure of the liquid such that it transitions into the gaseous state (saturated vapour), shown at point 2. The refrigerant then passes through a heat exchanger in contact with a body at a lower temperature, which cause it to condense and release heat, such that it becomes a saturated liquid. The expander then allows the refrigerant to return to its original lower temperature T_c as a liquid. Finally, between points 4 and 1 the refrigerant absorbs heat from a hotter body and begins to vaporise. While this cycle is theoretical and cannot be achieved in practice, it illustrates how heat can be transferred from a colder to a hotter body by a heat pump. A key point to note is that the refrigerant must have a sufficiently low evaporation temperature in order to function effectively.

In reality, heat pump cycles are more similar to that shown in Figure 2.2. Several differences can be observed between this cycle and that shown in figure 1. Firstly, the expander is replaced by an expansion valve in which the fluid undergoes an irreversible isentropic expansion. Secondly, the expansion process from 4-1 is allowed to continue to the saturated vapour line (i.e. all the refrigerant is in the gaseous state).
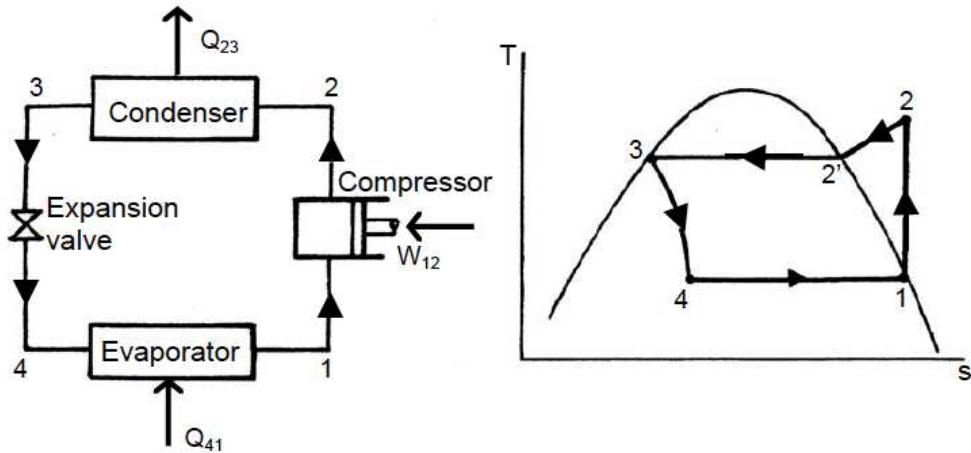
Figure 2.2: Practical vapour-compression cycle (Tuohy, 2013)

Higher energy efficiencies can be obtained by employing multistage cycles, so-called because they employ more than one compression stage, which can be further subdivided into compound and cascade systems. Examples of both are shown in Figure 2.3. A compound system employs two compressors which are connected in series, with intercooling between the compression stages. Compound systems offer smaller compression ratios, higher compression efficiency, a larger overall refrigeration effect and a lower discharge temperature after compression (Chua, 2010).
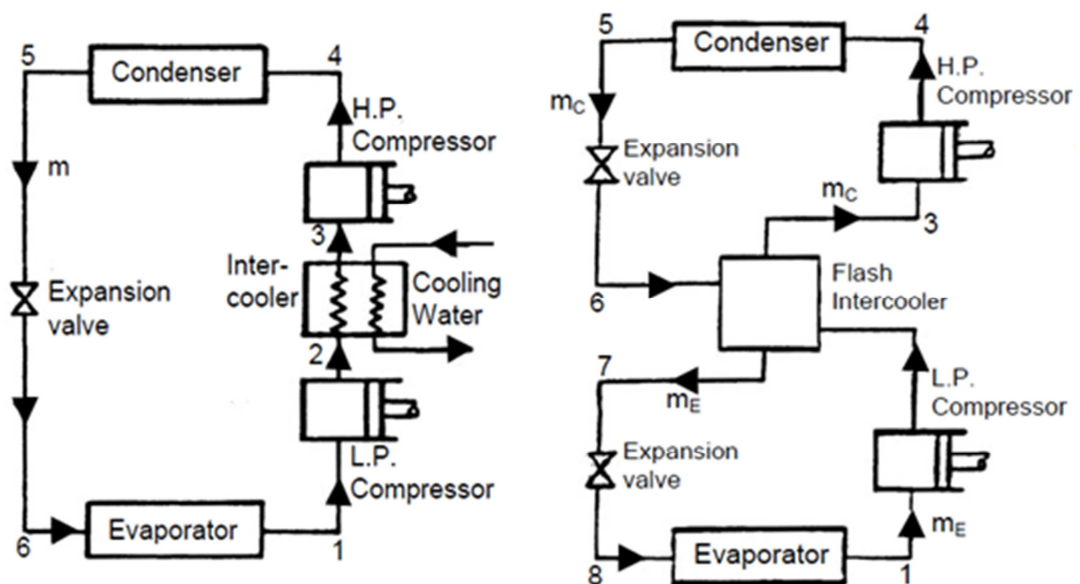
Figure 2.3: Two-stage vapour-compression cycles, compound cycle and cascade cycle (Tuohy, 2013)

14

A cascade cycle employs two single-stage refrigeration cycles. One cycle operates at a lower evaporating temperature, and this cycle removes heat from the body to be cooled. The other cycle operates at a higher evaporating temperature and heat is exchanged between the two cycles by an intermediate heat exchanger.

2.1.2 COP, SPF values and heat pump performance

The property by which the performance of a heat pump is evaluated is most commonly its coefficient of performance (COP). Put simply this value gives the ratio of heat added or removed (depending on whether heating or cooling) out of the system, to electricity consumed in operating it. Thus it is expressed simply:

$$COP = \frac{Q}{W}$$

Where Q is the heat added or removed from the system and W is the work performed by the system to remove this heat (i.e. in the form of a pump). The COP of a device is dependent upon whether it is used for heating or cooling, and can expressed according to the convention adopted in Figure 2.4:

$$COP_c = \frac{Q_1}{W}$$

$$COP_h = \frac{Q_2}{W} = \frac{Q_1}{W} + 1$$

Values of COP can varying significantly depending on both the exact nature of the system and the conditions under which it is operating. COP values quoted by manufacturers should have been obtained adhering to EN14511 (ECS, 2007) and values can vary significantly. Field trials conducted by the Energy Savings Trust showed that installations of GSHP systems in the UK had COPs of 1.3-3.6 (Energy Savings Trust, 2010). A more realistic assessment of heat pump performance is given by the seasonal performance factor (SPF). In contrast to a COP value, the SPF is calculated over the basis of an entire season, providing a much more relevant view of heat pump performance (IEA, 2013). An additional performance measure is that of system efficiency, which was developed by the Energy Savings Trust. This includes not just the heat pumps itself but the entire heating network, including additional pumping (of surface water in the case of a lake-based GSHP for example), and any backup heating required.
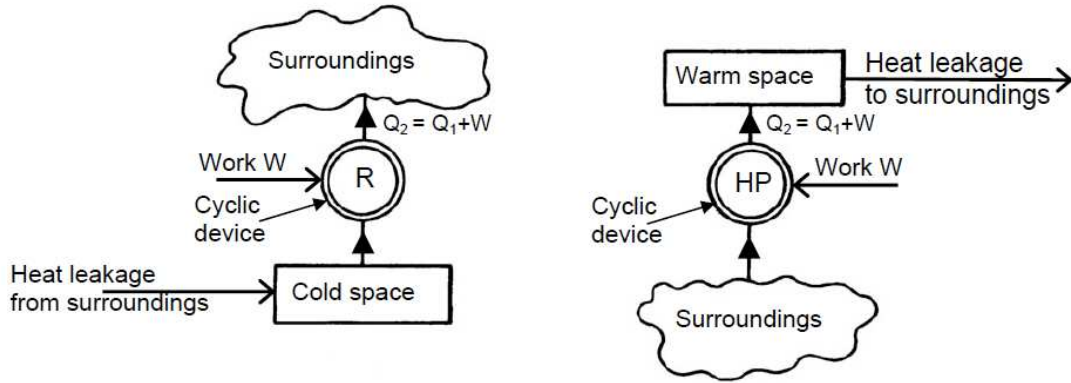
Figure 2.4: Operation of a refrigerator and heat pump (Tuohy, 2013)

Heat pump performance is highly dependent upon the temperature range in which it is required to operate (i.e. the temperatures at the evaporator and condenser). The COP for the ideal reversed Carnot cycle can be shown to be:

$$COP = \frac{T_C}{T_H - T_C}$$

It can therefore be seen that the COP of a heat pump will be maximised when operating between two temperatures with a small temperature difference. This means that heat pumps operating in colder climates are better suited to supplying heat at low temperatures, and are therefore best used for space heating by underfloor heating which requires lower temperatures of around 35°C compared to around 80°C for conventional wall-mounted radiators (Carbon Trust, undated).

2.2 Surface water GSHP

Surface water heat pumps utilise sources of water on the earth's surface, including lakes, ponds and rivers as sources of low-grade heat. Although the source of heat is in fact water and not the ground, heat pump systems of this kind are known as surface water GSHPs, as a distinction from air-source. Heat pumps of this kind can be broadly subdivided into closed- and open-loop systems.

2.2.1 Closed-loop schemes

In a closed-loop scheme, a heat transfer fluid (normally an antifreeze solution) passes through a heat exchanger and absorbs heat from the water body. This fluid then travels to the evaporator where the heat is given up to the heat pump evaporator. Such schemes are similar to those commonly buried underground in GSHP applications,

with the exception that thermal contact is made between the heat exchanger and water body rather than earth or rock. The amount of heat which can be extracted from such a scheme is limited by several factors, as given in Banks (2012). Namely, the short term limit is presented by the effectiveness of transfer between the water and the heat exchanger. In the longer term it is limited by the rate at which heat can be replenished to the body from which it is being taken, known as the thermal budget (Banks, 2012).

There are two primary means by which heat may be extracted from the system, either by coils of HDPE piping, or by flat plate heat exchangers (Banks, 2012). Images for both systems are shown in Figure 2.5 below. A slinky arrangement takes the form of a series of parallel and overlapping coils, commonly employed in GSHP applications since they can reduce the overall land area required (Energy Savings Trust, 2004). Alternatively, bundles of loose coil may be laid at the water bottom, normally affixed to a frame or within a wire cage. These arrangements can be seen to more suitable to man-made water-sources, where the pipes can be laid in place before water is added to the construction. Alternatively, coils may be affixed to a raft, floated out and subsequently sunk to the bottom of the water body. This last approach has been employed for example by a domestic project in the Lake District (R & M Wheildon Limited, 2012). Omer (2008) suggests that closed loop scheme require 26 m/kW of heat transfer piping, and around 79.2 m^2/kW of pond surface area.

Figure 2.5: Heat exchangers for closed-loop surface water heat pumps. Coiled HDPE piping affixed to a steel frame (left) and Slim Jim[TM] flat plate heat exchanger (right). Images taken from (Wheildon's, 2012), (AWEB Supply, 2013).

An alternative method which has been employed on a number of projects is the use of flat plate collectors, which offer a significantly lower heat exchanger area due to a higher heat transfer coefficient (Banks, 2012). The New Lanark Conservation Trust has installed three panels of this kind in a fast-flowing Mill lade after there was concern that a slinky type arrangement may have been sucked into a nearby turbine (The Green Blue, 2013). The performance of the plates has been found to be lower than claimed by the manufacturers, and additional plates were installed to meet demand – double the original area (Phillips, 2013). Flat plates were also adopted by the Clyde Maritime Trust in the River Clyde for the purpose of transferring heat to an 80kW heat pump scheme aboard the restored Glenlee tallship, now used as a visitors' attraction (The Scottish Government, undated).

In both of the above cases, Slim Jim™ plates were used. These plates are pre-fabricated steel or titanium plates, available in a number of sizes according to the application ranging from the SJ-02T with approximate dimensions of 0.6 m by 1.8 m to the SJ-10T with approximate dimensions 1.2 m by 4.6 m (AWEB Supply, 2013). Amongst the benefits cited by the manufacturer are easy installation and easy scalability – more plates can be easily added to a system in order to create greater capacity. Fluid input and output is normally by a single inlet and outlet, shown in Figure 2.6. Plates can be assembled into arrays by metal frames, and should be held above the lake floor to prevent sediment build up.

Figure 2.6: Four SJ-10T plates with inlet and outlet tubes (AWEB Supply, 2013)

2.2.2 Open-loop schemes

In an open-loop scheme, water is extracted from the source and heat is extracted before being returned at a colder temperature. Such a scheme will often require a submersible pump if the water body is greater than 5-6 m deep, otherwise a ground-mounted suction pump can provide adequate head and will prove more convenient to install and maintain (Banks, 2012). An additional consideration is the potential for debris, biofouling and corrosion in the piping and heat exchanger system. These issues can be managed with the use of filters on intake pipes, and with prophylactic heat exchangers which remove the risk of fouling from the heat pump evaporator and placing it instead on the heat exchanger.

In designing such systems it is important to site intake and outtake pipes sufficiently far away from one another in order to prevent what is described as thermal "short-circuiting", i.e. colder water from the system outlet mixes and is subsequently returned via the inlet, decreasing the COP. There is also a heightened risk of freezing in open-loop schemes, as water is cooled from low temperatures without the possibility of anti-freeze to prevent ice formation (Banks, 2012). Greater consideration must be given to the effects on animal life with an open-loop scheme, and licences may need to be sought for the extraction of water from a source (Stiebel Eltron, 2013). One of the first examples of water-based GSHP adoption in the UK was an open-loop scheme, extracting water from the River Wensum in Norwich. The plant room containing the main components of the heat pump is shown in Figure 2.7). Built in 1948, the system delivered a peak power of 243 kW (147 kW on average) and monitoring of the system showed an average COP of 3.45 (Sumner, 1948).
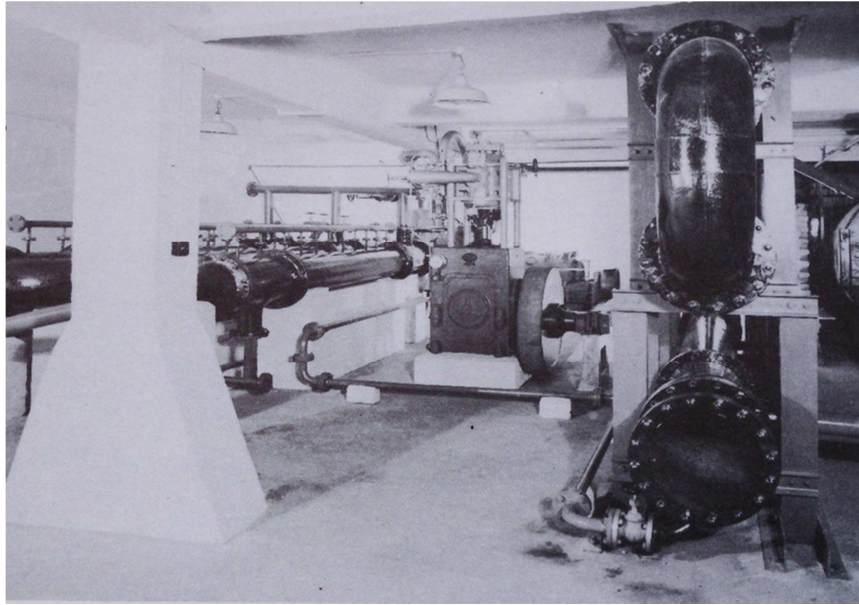
Figure 2.7: An early example of heat pump heat generation in the UK (Banks, 2012)

2.2.3   Comparison of closed- and open-loop schemes

The relative advantages and disadvantages of closed and open-loop schemes should be considered in the decision to pursue either such setup. In terms of energy efficiency there are several factors which should be considered. Closed-loop schemes will have greater energy losses associated with the carrier fluid as it travels from the water source to the heat pump evaporator, which are not encountered in an open-loop scheme (Banks, 2012). However, greater pumping power will be required for an open-loop scheme, since the static head associated with the lake depth must be considered. As stated previously, in cold climates open-loop schemes are at greater risk of freezing due to the lower volume of water used in the heat exchanger, and greater consideration must be given to corrosion and biofouling.

While it is generally accepted that open-loop schemes offer better energy efficiency due to the fact that heat is transferred directly from the source to the refrigerant, rather than through an intermediate heat exchange with a transfer solution, each case must be assessed individually and rules-of-thumb are not advisable or easily applied (Egg, 2011). A summary of the comparison between open and closed loop WSHP systems is given in Table 2.1.

	Closed-loop	Open-loop
Efficiency	May be lower due to temperature losses in transfer to closed loop, however pumping costs are low	No losses to a closed loop, but pumping energy must also be considered
Licensing	No extraction license required	Extraction license required for high volumes, discharge consent may also be required
Maintenance	Possible biofouling of heat exchanger, but no risk of corrosion at evaporator	Requirement for corrosion resistant equipment if pH non-neutral, water filtration also necessary
Ice formation	No risk of freezing at evaporator, though risk remains at heat exchanger in cold weather	Risk of freezing at evaporator at low temperatures

Table 2.1: Comparison of closed and open-loop WSHP schemes (YouGen, 2012)

An indication of possible system configurations is given in Figure 2.8. Note that the pink loops denote anti-freeze solution, the black loops denote the refrigerant loop, while blue loops indicate water loops. The first would be a conventional heat pump unit located in the site to be heated, supplied by an anti-freeze loop which would pass through the reservoir then into the site. This would require infrastructure in laying piping to carry the anti-freeze solution. The second system, known as a split-system, would employ a shorter anti-freeze loop, instead extending the heat pump refrigerant circuit such that an evaporator is placed beside the reservoir, while the condenser remains in the main site. Lastly and open-loop system is shown where water is extracted, passes through the evaporator and then is then ejected from the system.

2.2.4 Lake-based GSHP case studies

As has been previously mentioned, the heat source for a heat pump may take one of several forms. The use of a large body of water as a source offers key benefits: high thermal capacity and a good heat transfer medium (given the thermal conductivity of water is ~0.58 $Wm^{-1}K^{-1}$ compared to ~0.024 $Wm^{-1}K^{-1}$ for air and 0.15-2 $Wm^{-1}K^{-1}$ for soils). Several examples of the use of ponds and lakes as sources for heat pumps in the UK and elsewhere have been found and are described here.
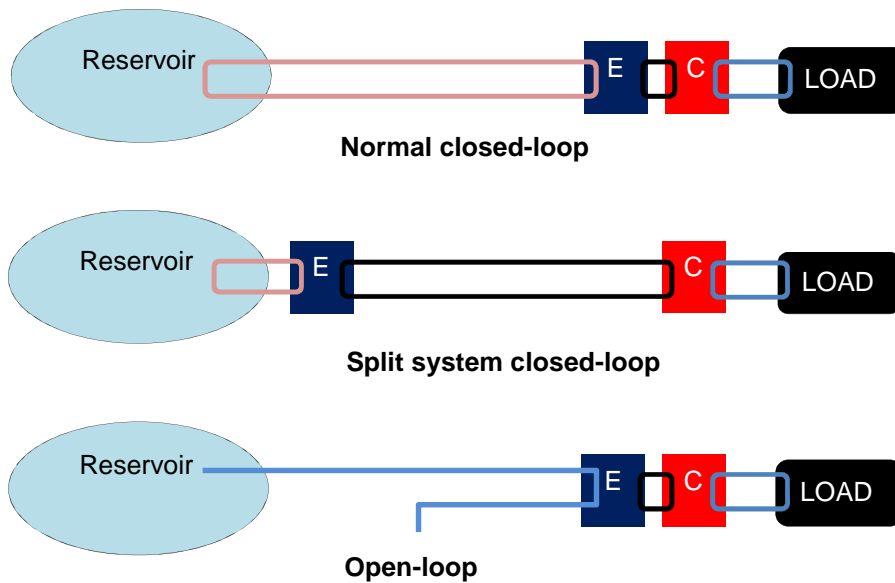
Figure 2.8: Configurations of closed- and open-loop WSHP schemes

King's Mill Hospital, Mansfield, UK

A lake-based GSHP scheme has been constructed in King's Mill hospital in 2008. The scheme is reported to be the largest of its kind in Europe, with a cooling capacity of 5.4 MW and a heating capacity of around 5 MW (Renew-Reuse-Recycle, 2009, Banks, 2012). A total of 45 heat pumps are employed on the site to provide hot water for space heating at 45^oC and chilled water at 6^oC for cooling. The heat source for the scheme is a lake with volume of approximately 825,000 m^2 (given its surface area of 165,000 m^2 and an approximate depth of 5 m), with annual temperature variations of 3-21^oC at the lake surface. The design temperature for the heat exchanger fluid used in the scheme is between -2-40^oC (winter-summer) and heat exchange takes place on 140 stainless steel flat plate "Slim Jim" exchangers, giving a total heat exchange surface area of 1560 m^2 (see Figure 2.9) . The scheme is quoted as savings 9,600 MWh of gas and electricity annually, and in terms of performance, seasonal performance values of between 4 and 7 have been achieved (i.e. the average COP over the heating season) (Banks, 2012)

Figure 2.9: Flat plate heat exchangers at King's Mill before being submerged (AWEB Supply, 2013)

Westport Lake Visitors Centre, Stoke-on-Trent

The Westport Lake is the largest body of water in the city of Stoke-on-Trent (Stoke-on-Trent City Council, 2013a), though an exact volume could not be sourced. The lakeshore includes a visitor centre which was completed in 2009 and includes as part of the design a GSHP operating on the lake (Stoke-on-Trent City Council, 2013b). An 11kW heat pump utilising 600 m of coiled heat exchanger piping was installed, providing low-temperature water for an underfloor heating system in addition to domestic hot water. The building includes a number of other technologies including solar thermal and PV systems and has had significant recognition for its design (Stoke-on-Trent City Council, 2013b).

Waterton Park Hotel, Wakefield, UK

Walton Hall near Wakefield is cited in the centre of a large 26 acre (105,219 m^2) lake on a man-made island (UFW Limited, 2013). An initial installation of a 60 kW heat pump for pool heating was installed, and after the scheme proved successful a further two 60 kW pumps and an additional 24 kW pump to heat the remainder of the leisure area, 17 guest rooms, bar, restaurant and meeting rooms via traditional wall-mounted radiators. Heat transfer in the lake is by 3200 m of weighted medium-density polyethylene (MDPE) piping. Monthly savings of around £3,500 have been cited by the hotel as a result of reducing oil consumption (UFW Limited, 2013).

Great River Medical Centre, West Burlington, Iowa

This large-scale project has been recognised as the largest water-source scheme in America, with a cooling capacity of around 5.3 MW (Alliant Energy, 2013). This includes around 132 km of pipe coils arranged in 105 grids in a purpose-built, 61,000 m^2 lake beside the hospital, serving 800 water-to-air heat pumps throughout the building. The array of heat exchanger coils is shown in Figure 2.10.

Figure 2.10: Aerial view of the heat exchanger array at Great River Medical Centre (KJWW Engineering Consultants, 2013)

2.3   Modelling of thermal reservoirs

In order to understand the performance of a heat pump operating with a body of water as a thermal reservoir, it is important to understand what is known as the "energy budget" of the water body. Several previous authors have developed mathematical models of reservoirs. The basic principles behind some of these models will now be discussed.

A Model for Simulating the Performance of a Shallow Pond as a Supplemental Heat Rejecter with Closed-Loop Ground-Source Heat Pump Systems, Chiasson, et al. (2000)

Chiasson, et al. (2000) developed a model of a shallow pond in the TRNSYS modelling environment (Type 230) to investigate its potential use as a heat rejecter for

a GSHP. The model is built on the lumped capacitance method, which implies the assumption that the pond can be treated as a single body with a uniform temperature. The fundamental guiding equation is expressed:

$$Q_{in} - Q_{out} = V\rho c_p \frac{dT}{dt}$$

where Q_{in} gives the heat transfer rate into the pond, Q_{out} is the heat transfer rate out of the pond, V is the volume of water in the pond, ρ is the water density, c_p is the specific heat capacity of the water and dT/dt is the rate of change of temperature of the water. A number of heat transfer mechanisms are considered in the model: solar gains; thermal radiant surface heat transfer; convective surface heat transfer; conductive transfer to the ground; transfer due to water inflow and outflow; evaporation at the surface and heat transfer from a fluid as part of the GSHP loop, and these are illustrated in Figure 2.11.
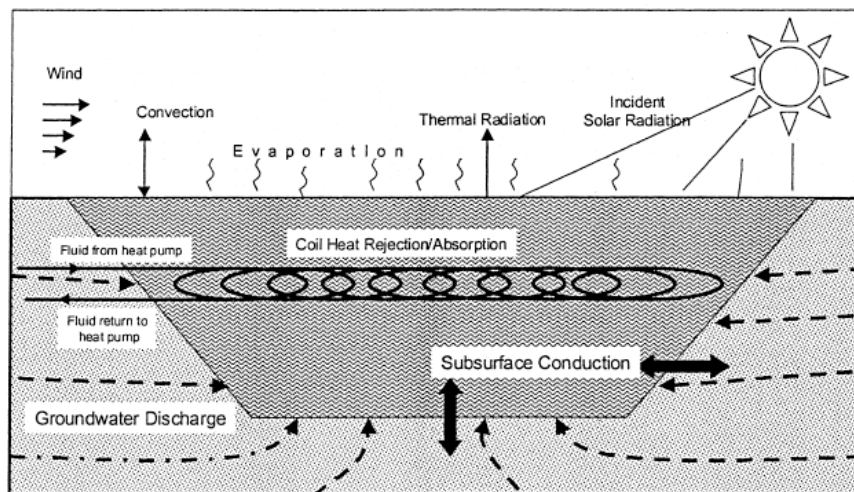
Figure 2.11: Energy flows for a thermal pond according to the model of Chiasson, et al. (2000)

Solar gains are expressed by the relation:

$$Q_{solar} = I(1 - \rho')A_{pond} \qquad (2.1)$$

where I is the incident solar flux A_{pond} the total pond area and ρ' is the reflectance. The value of ρ' is calculated according to the angle of solar incidence, which is calculated for each timestep of the model by relations given in Duffie and Beckman (1991). The incident solar flux is obtained from local weather data collected at 15 minute intervals.

Thermal radiation can account for a significant degree of cooling during the night (Chiasson, et al., 2000) and is accounted for by a linearised radiation coefficient (h_r), which is expressed:

$$h_r = 4\varepsilon\sigma \left(\frac{T_{pond} + T_{sky}}{3}\right)^3$$

Where ε is the emissivity coefficient of the water, σ is the Stefan-Boltzmann coefficient, T_{pond} is the surface temperature of the water and T_{sky} is the sky temperature which is calculated from a relation in Bliss (1961). The sky temperature can also be calculated by the relation found in Davies (2004):

$$T_{sky} = T_{air}\left(0.8 + \left(T_{dp} - 273\right)/250\right)^{1/4}$$

where T_{dp} is the dew point temperature at the given conditions. The heat transfer is then calculated by the relation:

$$Q_{thermal} = h_r A_{pond}\left(T_{sky} - T_{pond}\right)$$

Surface convection is also included, though Chiasson notes that this mechanism is less significant than other heat transfer mechanisms. For convective transfer the pond is modelled as a flat plate and the corresponding correlations for free and forced convection are used, namely:

$$\text{Nu} = 0.54\text{Ra}^{1/4} \quad (10^4 < \text{Ra} < 10^7 \text{ - laminar})$$

$$\text{Nu} = 0.15\text{Ra}^{1/3} \quad (10^7 > \text{Ra} > 10^{11} \text{ - turbulent})$$

Where Nu is the Nusselt number and Ra is the Rayleigh number which is calculated:

$$Ra = \frac{g\beta(\Delta T)L^3}{\nu\alpha}$$

Where g is the acceleration due to gravity, α is the thermal diffusivity, β is the volumetric thermal expansion coefficient and ν is the kinematic viscosity of air, ΔT is the temperature difference between the pond and air and L is the characteristic length. In the case of a plate the characteristic length is calculated by:

$$L = \frac{A_{pond}}{P_{pond}}$$

where P_{pond} is the total perimeter. In the model the terms α, β and ν are evaluated at the film temperature, which is the average temperature of the pond water and the air. These values were obtained from analytical relations presented in Irvine and Liley (1984). The convection coefficient is calculated from the relation:

$$h_c = \frac{\text{Nu}\,k}{L}$$

where k is the thermal conductivity of air at the film temperature. Forced convection is calculated in a similar fashion, and the larger convection coefficient is used to calculate the energy transfer by:

$$Q_{convection} = h_c A_{pond}(T_{air} - T_{pond}) \tag{2.2}$$

Heat transfer to the ground was calculated using an analytical expression developed by Hull, et al. (1984) which can be used to calculate the total U-value for the pond-ground interface by the relation:

$$U_{ground} = 0.99\left(\frac{k_{ground}}{d_{ground} - d_{pond}}\right) + 1.37\left(\frac{k_{ground}P_{pond}}{A_{pond}}\right)$$

$$Q_{ground} = U_{ground}A_{ground}(T_{groundwater} - T_{pond})$$

Where k_{ground} is the thermal conductivity of the ground, d_{ground} is the depth to the nearest heat sink, d_{pond} is the pond depth and $T_{groundwater}$ is the temperature of the constant heat sink. This assumes that the heat lost from the pond bottom is lost by transfer to the nearest constant temperature sink, taken to be the groundwater table.

Heat transfer by the addition or abstraction of water, which may be used to model both groundwater losses/addition or rainwater for example, is calculated from the expression:

$$Q_{water} = Q\rho c_p(T_{water} - T_{pond}) \tag{2.3}$$

Where Q is the volumetric flow rate of the water.

The major source of heat loss from the pond is evaporation. The model uses the j-factor analogy to calculate water mass loss by evaporation:

$$\dot{m}_w'' = h_d(w_{air} - w_{surf})$$

Where h_d is the mass transfer coefficient, w_{air} is the humidity ratio of the ambient air, w_{surf} is the humidity ratio of saturated air at the pond surface. The coefficient h_d is calculated by the Chilton-Colburn analogy as:

$$h_d = \frac{h_c}{c_p \text{Le}^{2/3}}$$

Where h_c is the convection coefficient as previously described, c_p is the specific heat capacity of air at the pond-air film temperature and Le is the Lewis number defined as:

$$\text{Le} = \frac{\alpha}{D_{AB}}$$

Where α is as previously defined and D_{AB} is the binary diffusion coefficient. The heat transfer by evaporation is then calculated by:

$$Q_{evaporation} = h_{fg} A_{pond} \dot{m}_w''$$

Where h_{fg} is the latent heat of evaporation. An additional term Q_{fluid} was also developed to calculate the heat transfer from the pond to the loop of the heat exchanger coil which is not discussed here.

The change in temperature of the pond is expressed by expanding and rearranging equation (1) shown previously to give:

$$\frac{dT}{dt} = \frac{(Q_{solar} + Q_{thermal} + Q_{convection} + Q_{ground} + Q_{groundwater} + Q_{evaporation} + Q_{fluid})}{V \rho c_p}$$

This can be seen to be of the form:

$$\frac{dT}{dt} = x_1 T + x_2$$

Where T is the pond temperature, x_1 represents all those heat transfer terms which multiply T and x_2 all those terms which do not. In the model this linear differential equation is solved at each timestep in order to obtain the new value of T.
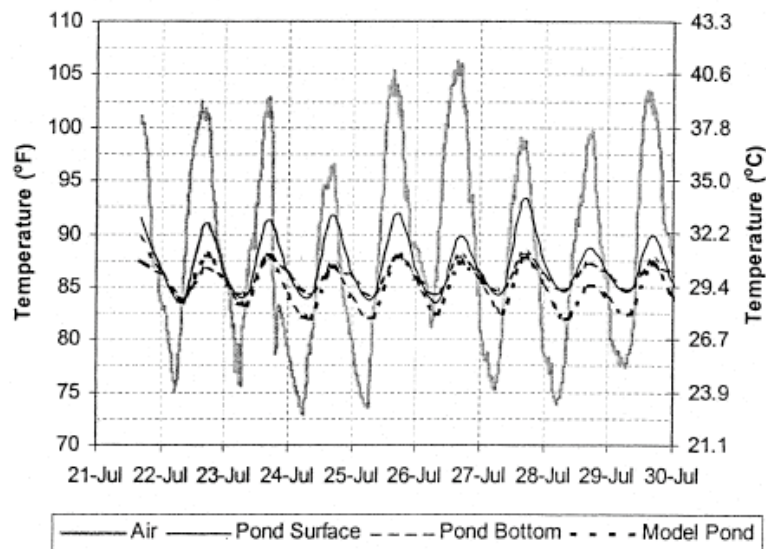
Figure 2.12: Validation results of the model presented in Chiasson, et al. (2000)

The Chiasson model was validated for the cases of both no heat rejection into the pond and with heat rejection into the pond and was shown to provide good agreement with measured pond temperatures over a week long period, see Figure 2.12.

Temperatures predicted by the model were within 1.67°C of the average pond temperature during the test period.

Heat Balance Analysis to Validate the Heat Dissipation Rate of a Man-Made Lake as a Heat Rejection Device in a Power Plant, Hayes, et al. (2012)

A similar but simpler model is presented by Hayes, et al. (2012). This model was developed to investigate the heat rejection rate to a lake used as a condenser by a gas power plant. The basic energy equation used in the model is given by:

$$\rho V c_p dT = Q_{convection} + Q_{conduction} + Q_{evaporation} + Q_{solar} + $$
$$Q_{emitted} + Q_{condenser}$$

In this model the heat transfer mechanisms considered are: natural convection at the lake surface; conduction through the lake bed; heat loss by surface evaporation; heat gain from solar radiation; radiative loss to the sky; heat gains from the power plant condenser.

Solar radiation is calculated by (2.1) as previously explained, but in this model the incident angle is determined by a method described in Hsieh (1986). The surface reflectivity is determined by a curve produced by Duffie and Beckman (1974) for a blackened surface.

Radiative losses are calculated by the equation:

$$Q_{emitted} = A\varepsilon_w \sigma \left(T_w^4 - T_{sky}^4\right)$$

Where all the symbols are as previously defined. However it is not clear how the sky temperature was determined in this model. An additional term was developed for condenser heat rejection into the pond $Q_{condenser}$ which will not be discussed here.

Convective transfer is determined by (2.2) as in the Chiasson model. However, the heat transfer coefficient h_c is obtained from tabulated values which give the value for different wind speeds. Where intermediate wind speeds were encountered linear interpolation was used.

Conductive transfer on the lake sides and bottom were not considered in this model, based on the findings of a previous model by Pezant and Kavanaugh (1990).

Evaporative losses were modelled by the method prescribed by the American Society of Heating, Refrigeration and Air-Conditioning Systems (ASHRAE 2009). The Carrier equation for energy lost by evaporation is expressed:

$$Q_{evaporation} = A(95 + 0.425v)(P_w - P_a)$$

Where A is the surface area of the pond, v is the velocity of the air (i.e. wind speed) and P_w and P_a are the saturation vapour pressure at the lake temperature and the partial vapour pressure of the ambient air.

The output of the model was validated by comparison of the lake water temperature predicted by the model with measured values over a 2.5 month period. Good agreement was observed between actual measured temperatures and those predicted by the model. In addition, the contributions of the various heat transfer mechanisms to the overall lake temperature were quantified (see Figure 2.13). It was observed that evaporation was the primary heat loss mechanism, with radiative and convective losses have much lower contributions to overall heat loss. It is important to note that model validation was performed using a large lake, with a surface area of 220 acres (890,308 m^2) and a depth of around 5 ft. Therefore care must be taken if applying this model to a lake of a significantly different size.
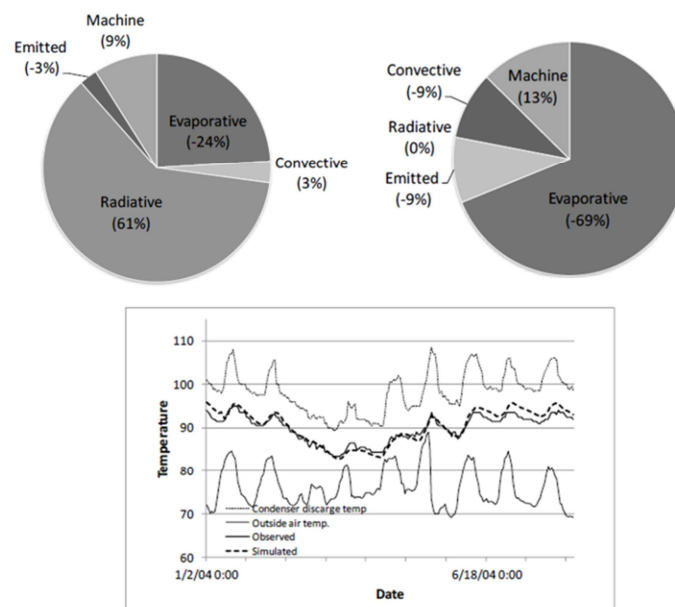
Figure 2.13: Results of the Hayes, et al. (2012), model showing relative contributions to heat transfer at (top left) noon and (top right) midnight in June. The lower graph shows the model validation results for the month of July.

An Introduction to Thermogeology: Ground Source Heating and Cooling, Banks (2012)

A third approach is presented by Banks (2012), who gives the main heat transfer mechanisms as: evaporative heat loss; sensible heat flux (comprising convective/conductive transfer with air); conductive transfer with the ground; short-wave solar and long-wave radiation from the clouds and atmosphere; reflective losses; back radiation from the water; advective heat fluxes comprising heat loss/gain from surface and ground water inflows and outflows.

Banks suggests that solar radiation reaching the pond can be found from literature sources, and that the albedo for short-wave radiation can be assumed to be between 6-10%, with lower values for long-wave radiation, as cited in Laval (2006).

Back radiation (i.e. thermal radiation emitted by the lake surface) is taken from Hostetler (1995) as:

$$Q_{back} = \varepsilon \sigma A (T_w)^4$$

Where the symbols are as previously defined.

The heat transfer due to addition or removal of water is defined by the basic equation (2.3) as adopted by Chaisson, et al.

Evaporative losses are said to be determined by either empirical relations based on local studies, basic theoretical relationships using Dalton's law, or by more theoretically based methods (perhaps such as that used by Chaisson, et al. (2000)). The rate of evaporation can be calculated according to a formulae derived by the US Geological Survey as:

$$E = 9.68 \times 10^{-4} v_{w8} (e_0 - e_a)$$

Here E is the evaporation rate in $m^3 s^{-1} m^{-2}$ (ms^{-1}), v_{w8} is the wind speed at 8 m above the water surface [ms^{-1}], e_0 is the saturated vapour pressure of water at the water surface temperature [Pa] and e_a is the vapour pressure of the surrounding air [Pa]. Banks notes that e_a is also equal to the vapour pressure of saturated air at the dew point temperature. If not known, the dew-point temperature can be calculated by the relation devised by Magnus-Teten:

$$T_{dp} = \frac{b\Omega}{a - \Omega}$$

Where:

$$\Omega = \left(\frac{aT}{b + T}\right) + \ln(RH)$$

Here T_{dp} is the dew point temperature [°C], $a = 17.27$, $b = 237.7$°C, T is the actual temperature and RH is the relative humidity expressed on a scale 0-1. The pressure e_0 can be calculated by the relation:

$$e_0 = 610.8 \times \exp\left[\frac{aT}{b+T}\right] \tag{2.4}$$

Therefore the value of e_a can be similarly calculated by replacing T with T_{db} in

$e_0 = 610.8 \times \exp\left[\frac{aT}{b+T}\right]$ (2.4) above.

From the calculation of the evaporation rate E, the energy loss can then be calculated:

$$Q_{evaporative} = \frac{AL_v\rho_w E}{86.4}$$

Where L_v is the latent heat of evaporation [MJ/kg] and ρ_w is the density of water [kg/L].

Sensible heat transfer between the air and the water is calculated based on the Bowen ratio, which is given as:

$$\text{Bowen ratio} = \frac{Q_{sens}}{Q_{evaporative}} \approx \frac{\psi_c(T_w - T_a)}{(e_0 - e_a)}$$

Here the term ψ_c is the psychometric constant in Pa/K where:

$$\psi_c = \frac{S_{Cair}P_{atm}}{0.622L_v}$$

In this term S_{Cair} is the specific heat capacity of air [J/kg], P_{atm} is the atmospheric pressure [Pa] and L_v is as previously defined.

Banks comments that heat fluxes with the ground can be largely ignored due to low thermal conductivity of geological materials and low temperature gradient between the ground and water in the reservoir (Banks 2012).

A long-term thermal equilibrium temperature can then be established by solving the energy balance:

$$Q_{evaporative} + Q_{back} \pm Q_{sens} + Q_{hp} = Q_{solar}$$

Where it has been assumed that the ground and surface water flows into the lake are negligible.

In this section, a literature review was performed in order to determine the basic operation of heat pumps and how performance is measured, the specifics of surface water GSHPs and their operation in closed- and open-loop schemes. Finally a number of mathematical models developed to investigate the temperature behaviour of a water body were summarised. The next chapter will proceed to explain the methodology adopted in this project, including a description of the site and of the mathematical model developed to represent both the reservoir and the heat pumps.

Heat transfer mechanism	Chiasson, et al. (2000)	Hayes, et al. (2012)	Banks (2012)
Solar radiation	$Q_{solar} = I(1 - \rho')A_{pond}$ *I* from local weather data, ρ' by calculation	$Q_{solar} = I(1 - \rho')A_{pond}$ *I* from local weather data, ρ' from curve	$Q_{sw} = A_{pond} R_{ex}\left(a + b\dfrac{n}{D}\right)$ n = actual hours of direct sun D = number of daytime hours R_{ex} = extra-terrestrial irradiance a, b = constants in Linacre (1992) $Q_{lw} = (258 + 3T_{sur})A_{pond}$ In both cases is ρ' constant at 0.08.
Thermal radiation	$Q_{thermal} = h_r A_{pond}(T_{sky} - T_{pond})$ $h_r = 4\varepsilon\sigma\left(\dfrac{T_{pond} + T_{sky}}{3}\right)^3$ where T_{sky} is calculated: $T_{sky} = T_{air}(0.8 + (T_{dp} - 273)/250)^{1/4}$	$Q_{emitted} = A\varepsilon_w\sigma(T_w^4 - T_{sky}^4)$ the source of T_{sky} is unknown	$Q_{back} = \varepsilon\sigma A(T_w)^4$ T_{sky} assumed to be zero
Convection with air	$Q_{convection} = h_c A_{pond}(T_{air} - T_{pond})$ where h_c is the larger of either forced or natural convection coefficients	$Q_{convection} = h_c A_{pond}(T_{air} - T_{pond})$ where h_c is taken from tabulated values for various wind speeds (linear interpolation)	$Q_{sens} \approx Q_{evaporative}\dfrac{\psi_c(T_w - T_a)}{(e_0 - e_a)}$ N.B. author notes this relationship is not applicable in areas of high wind speed
Conduction to ground	$U_{ground} = 0.99\left(\dfrac{k_{ground}}{d_{ground} - d_{pond}}\right) + 1.37\left(\dfrac{k_{ground}P_{pond}}{A_{pond}}\right)$ $Q_{ground} = U_{ground}A_{ground}(T_{groundwater} - T_{pond})$	Not considered	Not considered
Water addition/abstraction	$Q_{water} = Q\rho c_p(T_{water} - T_{pond})$	Not considered	$Q_{water} = Q\rho c_p(T_{water} - T_{pond})$
Evaporation	$Q_{evaporation} = h_{fg}A_{pond}\dot{m}_w^{"}$ j-factor model: $\dot{m}_w^{"} = h_d(w_{air} - w_{surf})$ Chilton-Colburn: $h_d = \dfrac{h_c}{c_p \text{Le}^{2/3}}$, $\text{Le} = \dfrac{\alpha}{D_{AB}}$	$Q_{evaporation} = A(95 + 0.425v)(P_w - P_a)$	$Q_{evaporative} = \dfrac{AL_v\rho_w E}{86.4}$ $E = 9.68 \times 10^{-4} v_{w8}(e_0 - e_a)$

Table 2.2: Summary of heat transfer equations used in thermal reservoir models

3 Methodology

In the following section, a basic description of the Guardbridge site, and more specifically of the reservoir will be presented. This will be followed by a description of the mathematical modelling performed, including the equations used to capture the physical processes in action, the platform used, and the sources for climatic and environmental data. It will conclude with a description of the methodology used to capture heat pump performance across a range of temperatures in the model.

3.1 Site description

The former Guardbridge Paper Mill is located in the village of Guardbridge, approximately 12km south-east of the city of Dundee and 7km west of the town of St Andrews in Fife, Scotland. The paper mill operated on the site from 1872-2008, having originally being built as a distillery (RCAHMS, 2011). In 2008 the site was purchased by the University of St Andrews, which plans to develop a low carbon energy centre incorporating laboratories, spin-out companies and a number of renewable and low-carbon energy technologies. This project forms part of the feasibility study into potential technologies to be used on-site. The site includes the Guardbridge Mill Loch Reservoir, which is located approximately 500m northwest of the main site (see Figure 3.1).
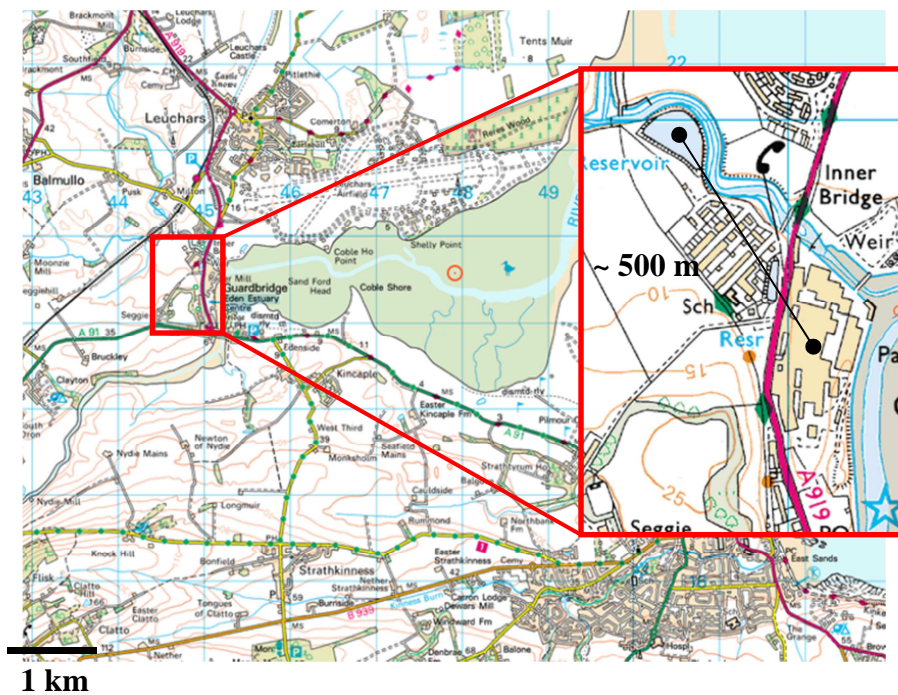
Figure 3.1: Guardbridge site location (Ordnance Survey, 2012)

Figure 3.2: View of the former Guardbridge Paper Mill (DC Thomson & Co., 2013)

Size and dimensions

The Guardbridge Mill Loch Reservoir was constructed in 1887 and has a quoted volume of $30927m^3$. The approximate dimensions of the reservoir are shown in **Figure 3.3**: Aerial view of the reservoir (Google Earth, 2013)below. Historical records show that the water level has been held between 6-8 ft, but that as of April 2013 was at around 6 ft (1.8288m). The maximum level is quoted at 10' 6" (3.2 m). The total surface area of the reservoir is quoted as 11,500 m^2 although this will vary according to the water level (University of St Andrews, 2004). In all analysis performed the surface area is assumed to be fixed at 11,500 m^2. Images of the reservoir site are shown in Figure 3.4.
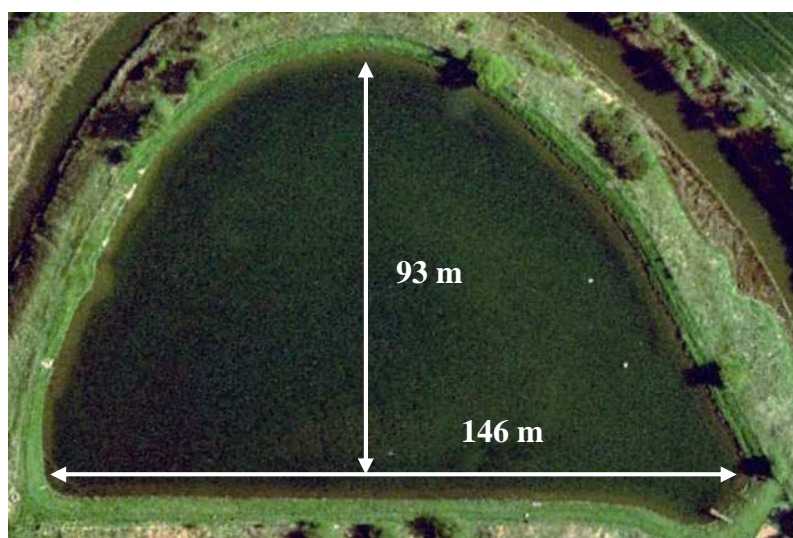
Figure 3.3: Aerial view of the reservoir (Google Earth, 2013)

Figure 3.4: Views of Guardbridge Mill Reservoir from the South and West

Construction

The reservoir lining is known to be clay, and a report of April 2013 says that no obvious leakage could be detected (Halcrow, 2013). The historical diagram shown in Figure 3.5 indicates that there is an inner lining of brick with a further lining of "puddled clay". This material has a very low hydraulic conductivity which makes it extremely watertight.
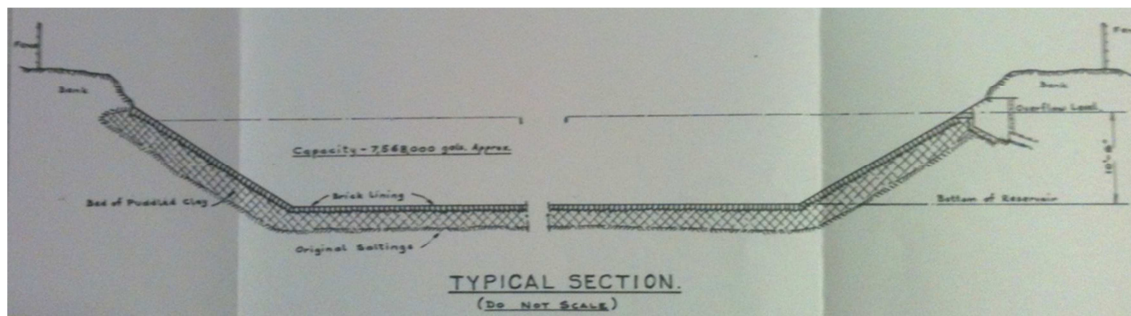
Figure 3.5: Historic record of the reservoir section

Water source and destination

The reservoir is supplied with water from a mill lade fed by the Motray Water, which has been dammed upstream, and a 14 in. and 12 in. pipe were subsequently installed to take water from the dam to the reservoir. Together these inflow pipes are estimated to provide a maximum flow of 0.18 m^3s^{-1}. Water abstraction from the reservoir is by an 18 in. pipe which takes water directly from the reservoir to the filter house on the Guardbridge site. The flow rate delivered by this abstraction pipe is quoted as also being 0.18 m^3s^{-1}. Water can also be taken directly from the Motray Water to the filter house via a bypass (see Figure 3.6).
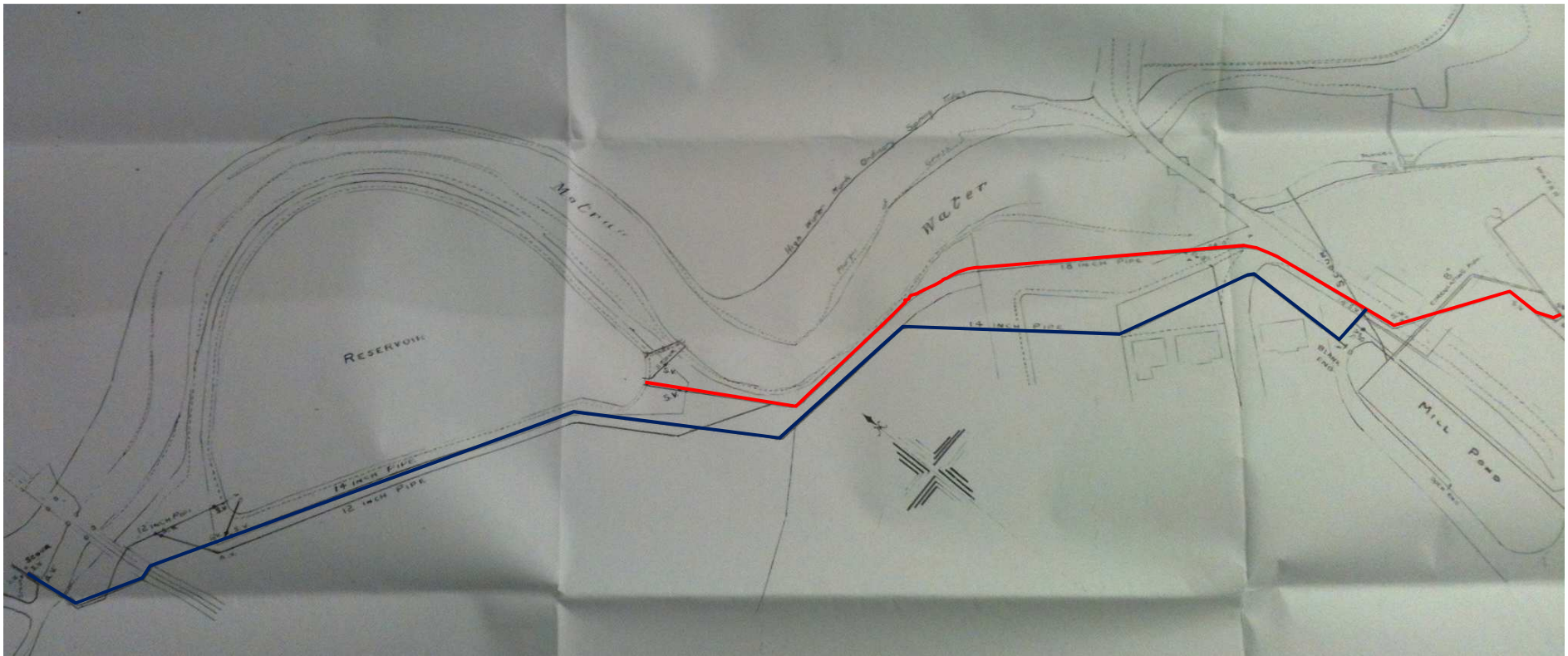
Figure 3.6: Reservoir piping network. The 18 in. pipe from the reservoir to the filter house is marked in red, and the bypass in blue

3.2 Thermal modelling of reservoir

An hourly timestep simulation was developed around the reservoir to predict the hourly temperature variation across a typical year. This program would then be used to evaluate the performance of a heat pump operating with the reservoir as a temperature source.

3.2.1 Theoretical basis

As previously discussed in section 2.3, there are a number of important heat flows associated with the reservoir. The model developed for this study takes into account heat transferred by: solar radiation; thermal radiation; evaporation; sensible transfer and water addition/abstraction. The theoretical basis for the calculation of each of these terms will now be discussed. These equations were chosen for the simplicity in their application, while capturing the key behaviours and energy flows within the reservoir.

Solar radiation

Radiation from the sun is the main source of heat for a water body such as a reservoir. The energy supplied to the reservoir by direct and diffuse radiation is calculated by the formula:

$$Q_{solar} = A_{reservoir}(1 - \rho')I \qquad (3.1)$$

Here $A_{reservoir}$ is the surface area of the reservoir [m^2], ρ' is the reflectivity of the reservoir surface and I is the global incident solar radiation (i.e. direct and diffuse) [Wm^{-2}]. As has been previously mentioned in section 2.3, the reflectivity of the reservoir to incident light is dependent upon both the nature of the light and the incident angle at the air-water boundary (Duffie and Beckman, 1991). The reflectance is given by:

$$\rho = \tau_a - \tau$$

Where τ is the transmittance of solar radiation by the surface of the reservoir and τ_a is the absorbance of the water. This is calculated by the relation:

$$\tau_a = e^{\frac{-\mu d}{cos\theta_r}}$$

Where μ is the extinction coefficient for water, d is the pond depth [m] and θ_r is the angle of refraction of the solar rays at the surface of the reservoir. The angle of refraction is calculated by Snell's Law:

$$\theta_r = sin^{-1}\left(sin\theta_i \frac{n_{air}}{n_w}\right)$$

Where n_{air} and n_w are the indexes of refraction for air and water, and θ_i is incident angle of the light on the reservoir surface. This value is taken from internal calculations performed in the TRNSYS weather module routine, which uses ASHRAE correlations (Chiasson, et al., 1999). The transmittance τ is calculated by the relation:

$$\tau = \frac{1}{2}\left(\frac{1 - r_\parallel}{1 + r_\parallel} + \frac{1 - r_\perp}{1 + r_\perp}\right)e^{\frac{-\mu' d}{cos\theta_r}}$$

Where $r_\parallel$ and $r_\perp$ are the parallel and perpendicular components of the unpolarized radiation, calculated from:

$$r_\parallel = \frac{tan^2(\theta_r - \theta)}{tan^2(\theta_r + \theta)}$$

$$r_\perp = \frac{sin^2(\theta_r - \theta)}{sin^2(\theta_r + \theta)}$$

Thermal radiation

A body with a finite temperature will emit longwave thermal radiation to its surroundings. In the case of a reservoir, the energy transfer can be considered to be between the water surface and the sky. It can therefore be calculated by the relation:

$$Q_{thermal} = A_{reservoir}\sigma\varepsilon_w\left(T_w^4 - T_{sky}^4\right) \tag{3.2}$$

Here $A_{reservoir}$ is as previously defined, σ is the Stefan-Boltzmann constant [kg s^{-3} K^{-4}], ε_w is the emissivity of water, T_w is the water temperature [K] and T_{sky} is the sky temperature [K]. The emissivity of water is taken as 0.97 for all calculations as documented by Robinson and Davies (1972). Sky temperature values are taken from processing climate data through the TRNSYS weather component Type 15-3.

Evaporation

Evaporation from the water surface has been shown to contribute significantly to heat losses from a reservoir (Hayes, et al., 2012). In the model, energy lost by evaporation is calculated by the relation (Banks, 2012):

$$Q_{evaporation} = 11.57L_v\rho_w E A_{reservoir}$$

Here L_v is the latent heat of vaporisation of water [kJ kg^{-1}], ρ_w is the density of water [kg L^{-1}], E is the evaporation rate [mm day^{-1}] and $A_{reservoir}$ is as previously defined. The evaporation rate can be calculated according to the analytical formula developed by the US geological survey as (Banks, 2012):

$$E = 9.68 \times 10^{-4} v_{w8}(e_0 - e_a)$$

Here v_{w8} is the wind speed at a height of 8 metres from ground level [ms^{-1}], e_0 is the saturation water pressure [Pa] and e_a is the actual vapour pressure at ambient temperature [Pa]. The saturation vapour pressure and water vapour pressure can be calculated based on the relations (Banks, 2012):

$$e_a = 610.8 e^{\left(\frac{aT_{air}}{b+T_{air}}\right)}$$

$$e_0 = 610.8 e^{\left(\frac{aT_{dp}}{b+T_{dp}}\right)}$$

Here T_{dp} is the dew-point temperature taken directly from weather data, a and b are constants with the values 17.27 and 237.7^{o}C and RH is the relative humidity expressed between 0-1.

Sensible transfer

Heat transfer between the air and the water is quantified by the Bowen ratio, which describes the ratio of heat transfer by sensible and evaporative mechanisms for water bodies to air (Banks, 2012):

$$\text{Bowen ratio} = \frac{Q_{sensible}}{Q_{evaporation}} \approx \frac{\psi_c(T_w - T_{air})}{(e_0 - e_a)}$$

Here ψ_c is the psychometric constant and can be assumed to take a value 65.95 Pa K^{-1} at atmospheric pressure. The total sensible heat transfer can be expressed then:

$$Q_{sensible} = Q_{evaporation}\psi_c \frac{(T_w - T_{air})}{(e_0 - e_a)}$$

Water addition

Water may be added to the reservoir from another water body, such as the mill lade. This is accounted for the in the model by an additional heat transfer term which is calculated:

$$Q_{water} = q\rho_w c_{p,water}(T_{river} - T_w)$$

Where q is the volumetric flow rate [m^{3}s^{-1}], $c_{p,air}$ is the specific heat capacity of water [J kg^{-1} K^{-1}] and T_{river} is the temperature of the river water.

Reservoir loop heat exchanger – Slim Jim$^{\text{TM}}$

Heat transfer between the reservoir and the Slim Jim$^{\text{TM}}$ heat exchanger plates can be modelled as natural convection on a vertical flat plate. The Rayleigh number is calculated by:

$$Ra = \frac{g\beta(\Delta T)L^3}{\nu\alpha}$$

Where g is the acceleration due to gravity [ms^{-2}], β is the volumetric thermal expansion coefficient [K^{-1}], ΔT is the temperature difference between the ice surface and the ambient air [K], ν is the kinematic viscosity [m^{2}s^{-1}], α is the thermal diffusivity [m^{2}s^{-1}] and L is the characteristic length [m] which in this case is the vertical height of the heat exchanger (=1.292 m for a SJ-10T plate). The Prandtl number is calculated by:

$$Pr = \frac{c_p\mu}{k}$$

Where c_p is the specific heat capacity of water [J kg^{-1} K^{-1}], μ is the dynamic viscosity [kg m^{-1}s^{-1}], equal to the water density multiplied by the kinematic viscosity, and k is the thermal conductivity [Wm^{-1}K^{-1}]. According to Incorpera, et al., (2007) the Nusselt number for a vertical flat plate can be calculated by:

$$Nu = \left(0.825 + \frac{0.387 Ra^{1/6}}{\left[1 + \left(\frac{0.492}{Pr}\right)^{9/16}\right]^{8/27}}\right)^2$$

The heat transfer coefficient h_{he} can then be calculated by:

$$h_{he} = \frac{Nu\, k}{L}$$

All fluid properties in the above calculations are evaluated at the film temperature which is given by:

$$T_{film} = \frac{T_w + T_{fluid,ave}}{2}$$

Where $T_{fluid,ave}$ is the average temperature of the anti-freeze fluid and is given by:

$$T_{fluid,ave} = \frac{T_{fluid,in} + T_{fluid,out}}{2}$$

Where $T_{fluid,in}$ is the temperature of the anti-freeze as it enters the heat exchanger and $T_{fluid,out}$ is the temperature as it leaves the heat exchanger.

The heat transferred to the anti-freeze solution is then calculated by:

$$Q_{fluid} = h_{he}A_{he}\left(T_{reservoir} - T_{fluid,ave}\right)$$

Where A_{he} is the total heat exchanger area. It should be noted that in order to determine the average fluid temperature in order to determine the heat transfer, the fluid outlet must be known. Therefore an iterative process must be undergone whereby the value of $T_{fluid,out}$ is assumed, and then refined in steps until the following condition is met:

$$\left|h_{he}A_{he}\left(T_{reservoir} - T_{fluid,ave}\right) - c_{p,g}\dot{m}_g\left(T_{fluid,out} - T_{fluid,in}\right)\right| < 5000$$

Where $c_{p,g}$ is the specific heat capacity of the glycol solution and $\dot{m}_g$ is the mass flow rate through the heat exchanger.

The energy transferred to the heat pump evaporator $Q_{heatpump}$ is calculated by the empirical relations given in Table 3.1, and is discussed in section 3.3.2. The fluid return temperature to the heat exchanger is then given by:

$$T_{fluid,in} = T_{fluid,out} - \frac{Q_{heatpump}}{c_{p,g}\dot{m}_g}$$

Here $c_{p,g}$ is the specific heat capacity of the glycol solution [Jkg⁻¹K⁻¹], which is calculated according to MEGlobal (2008) as:

$$c_{p,g} = 4186.8(0.89889 + 5.1554 \times 10^{-4}T)$$

It should be noted that it has been assumed that the heat transfer process with the greatest thermal resistance is that between the reservoir water and the heat exchanger surface, and as such, transfer through the exchanger walls and between the exchanger inner surface and the anti-freeze fluid is not considered. This is justified since the heat transfer by natural convection is known to be significantly lower than that by forced convection as will be experience in the heat exchanger, and the walls of the heat exchanger can be assumed to be thin and thus conduction will be negligible. The density of the glycol-water solution is assumed to have the same density as water at the same temperature. This is justified as the specific gravity of 30% ethylene glycol solution in the expected temperature ranges differs by only around 5% (Engineering Toolbox, 2013).

Energy balance

The change in temperature of the reservoir can be expressed:

$$\frac{dT}{dt} = \frac{\left(Q_{solar} \pm Q_{sensible} - Q_{thermal} - Q_{evaporation} + Q_{water} - Q_{fluid}\right)}{V\rho c_p}$$

The model calculates the heat transfer terms based on the reservoir temperature at the previous timestep T_t, then calculates the new temperature by the relation:

$$T_{t+\Delta T} = T_t + \frac{\left(Q_{solar} \pm Q_{sensible} - Q_{thermal} - Q_{evaporation} + Q_{water} - Q_{fluid}\right)}{V\rho c_p}$$

The heat transfer processes surrounding the pond are illustrated in Figure 3.7 overleaf.
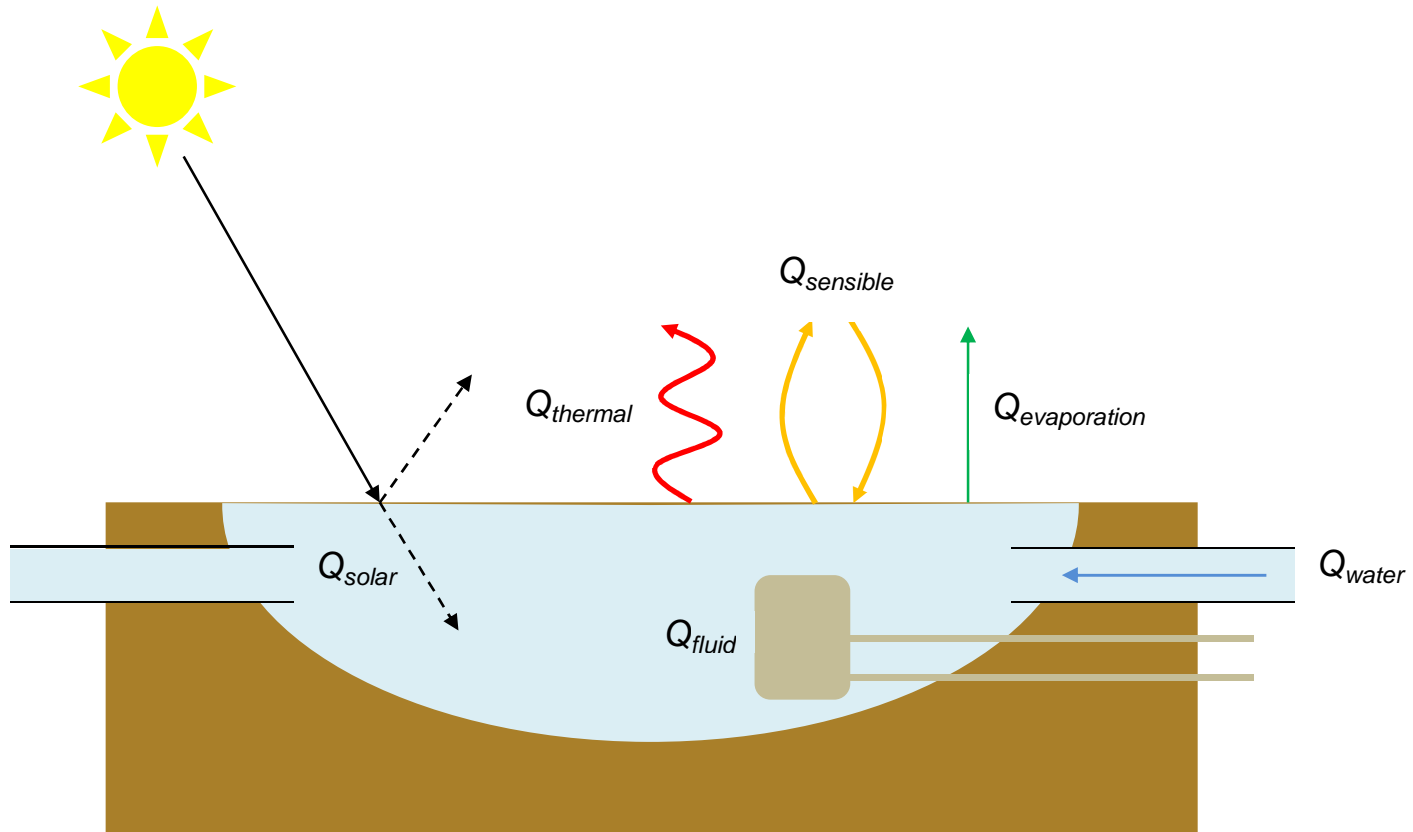
Figure 3.7: Energy flows around the model reservoir
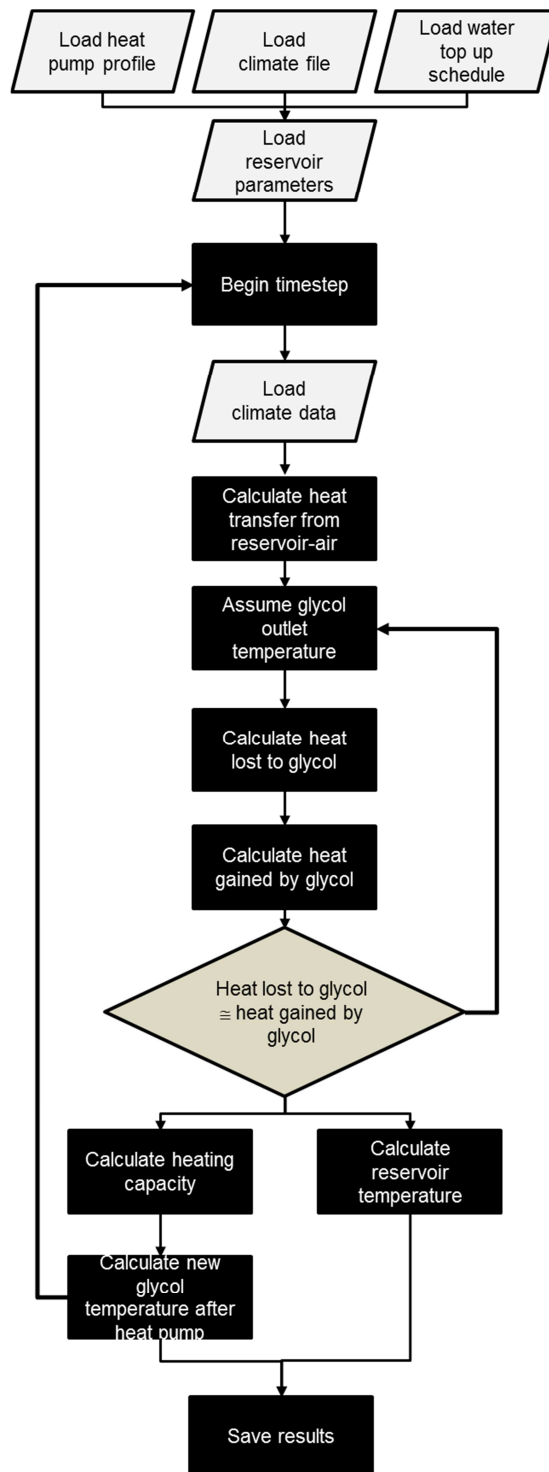
Figure 3.8: Flow chart denoting general logic of the reservoir temperature model

3.2.2 Program platform

The program was created in the open source Freemat environment (Freemat, 2013). The software is free to download and run and has a structure similar to that of the commercial MATLAB package. The platform was chosen due to its relative ease of use and flexibility. Copies of the various versions of the code used in the project can be found in appendixes 6.1 and 6.2. Versions of the material properties calculations used are given in appendix 6.3. The general program algorithm is shown in Figure 3.8.

3.2.3 Climate data

Data for this model has been acquired using the International Weather for Energy Calculation (IWEC) files available at the Energy Plus website for the weather monitoring station at RAF Leuchars (U.S. Department of Energy, 2012). These files are created using hourly weather measurements taken for up to 18 years, and solar data estimated from Earth-Sun geometry and weather conditions such as cloud cover. Sky temperatures were calculated using the TRNSYS weather module based on the same IWEC weather file as an input.

River temperatures were acquired for the Motray Water at a monitoring station ~ 2.5 km from the reservoir, at Burnside Cottage, St Michaels (NO44033 22381). Monthly temperature measurements were acquired from the Scottish Environment Protection Agency (SEPA) for the years 2000-2012 and averages of all data taken to give an average monthly temperature profile (SEPA, 2013). A polynomial curve was then fitted to the monthly data in order to give an approximate hourly temperature profile. Water flow rate for the Motray water was obtained from National Environment Research Council (2013). Daily flow rate measurements were obtained for the years 2000-2012 and averaged to approximate a "typical" annual flow rate profile.

The location of the weather monitoring station and river monitoring point relative to the reservoir are shown in Figure 3.9. The Motray water monthly temperatures and daily flow rates are illustrated in Figure 3.10.

Figure 3.9: Position of Motray water monitoring point (1) and RAF Leuchars weather station (2)
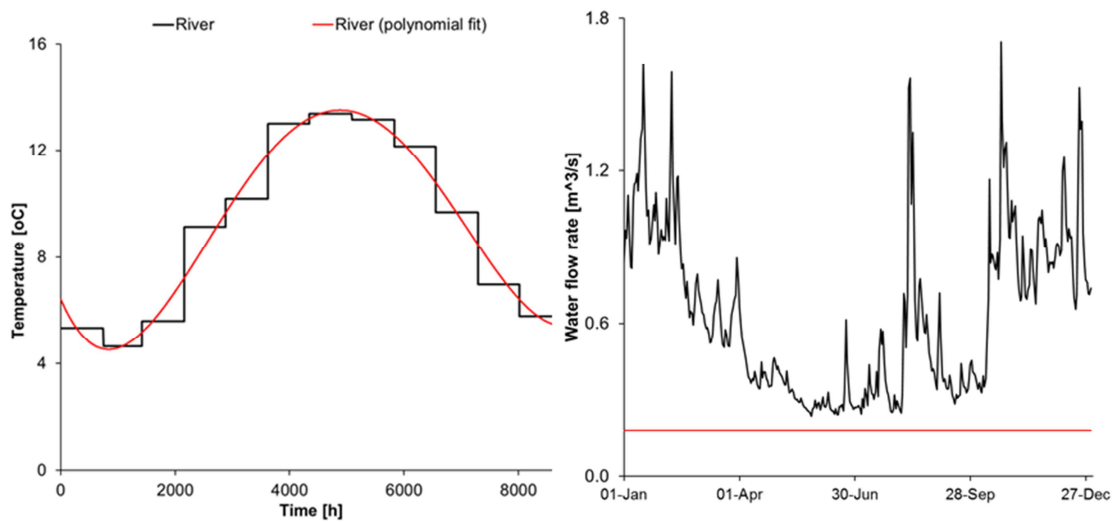
Figure 3.10: Motray water monthly river temperatures and polynomial curve fit, and river flow rate data (averaged over 2000-2012). The horizontal red line shows the maximum flow rate into the reservoir as quoted in the Reservoir Act log book

3.3 Heat pump integration

3.3.1 Heating demand profile

The heating schedule of the Guardbridge site will be determined by the pattern of occupation of the site buildings, however a general assumption is made that it will follow fairly standard working hours, with additional time in the morning in which to bring the initial building temperature to the temperature set point. A typical schedule is assumed to take the form shown in Figure 3.11. Heating operation begins at 7.00 in order to reach the temperature set-point for the start of the working day at 9.00, and continues operation until 18.00.

A general figure for the annual heating demand at the Guardbridge site has been estimated at 3842 MWh (Yarr, 2013). This equates to approximately 397 kW as a base heating demand across 12 months. In reality this will not be evenly distributed however, and demand will be higher in winter than summer. A more accurate determination of the peak heating was outwith the scope of this project.
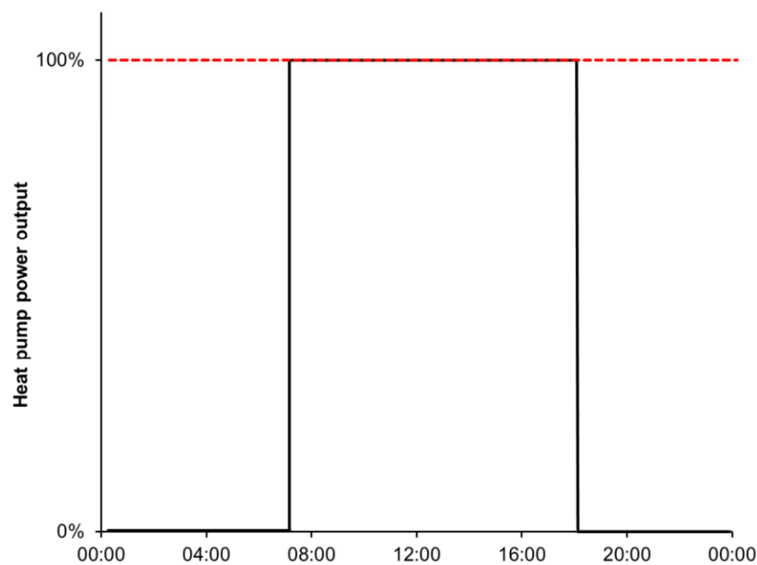
Figure 3.11: A typical office heating schedule

3.3.2 Heat pump performance

Heat pump performance was modelled on the Climaveneta RECS-W series of reversible water source heat pumps. This unit is available in a range of nominal heating capacities from 187 – 860 kW, and cooling capacities 174 – 801 kW. Manufacturer's technical data was used to generate data for typical COP and heating capacity for three different models, the RECS-W 0802 (187 kW), 1902 (468 kW) and 3202 (860 kW). Performance data for these three models was obtained from the manufacturer's website (Climaveneta, 2013). Additional data for performance outwith the temperature ranges provided by the manufacturer's literature were obtained by manufacturers software and provided by Young (2013).

In order to assess heat pump performance, condensing temperatures of 35°C and 50°C are assumed, representing what might be considered a 'low' output temperature, perhaps for direct underfloor heating, and a 'high' output temperature for integration into another heating network or for use in modern low-temperature radiator heating systems. Figure 3.12 shows the COP and the heating capacity at both condensing temperatures for a range of evaporator entering temperatures for all three models. Using known data points, a linear interpolation is used to derive empirical relations between the evaporator entering temperature and the COP and heating capacity of the heat pump. These empirical relations were then used as the basis for estimating heat pump performance for a range of evaporator temperatures. Note that in the case of an open loop system the evaporator temperature is simply that of the reservoir water, whereas for a closed loop system it is the temperature of the glycol solution after circulation through the heat exchangers in the reservoir.

A fixed volumetric flow rate is assumed for each model, based on the manufacturer's quoted value. Summaries of the empirical relations derived and the volumetric flow rates for each model are given in Table 3.1.

Heat pump model	Volumetric flow rate [m³h⁻¹]	Condenser temperature [oC]	COP relation (COP =)	Heating capacity relation $Q_{heatpump}$ [kW]
0802	24.7	35	$0.1262T_{in} + 3.8461$	$6.4485T_{in} + 134.1$
		50	$0.0872T_{in} + 2.6803$	$6.0486T_{in} + 120.16$
1902	61.1	35	$0.1203T_{in} + 3.8227$	$15.709T_{in} + 334.34$
		50	$0.0817T_{in} + 2.6543$	$15.014T_{in} + 303.26$
3202	114	35	$0.1266T_{in} + 3.9645$	$29.092T_{in} + 618.1$
		50	$0.0864T_{in} + 2.7764$	$27.223T_{in} + 556.46$

Table 3.1: Empirical relations for estimating heat pump performance

In this section, the methodology taken in the project has been discussed, including a description of the site under investigation, and a summary of the mathematical basis and implementation of a thermal model of the reservoir. It concluded with a discussion of the approach taken to assess heat pump performance across a range of temperatures. The results of the modelling performed will be presented in the following section.

RECS-W 0802
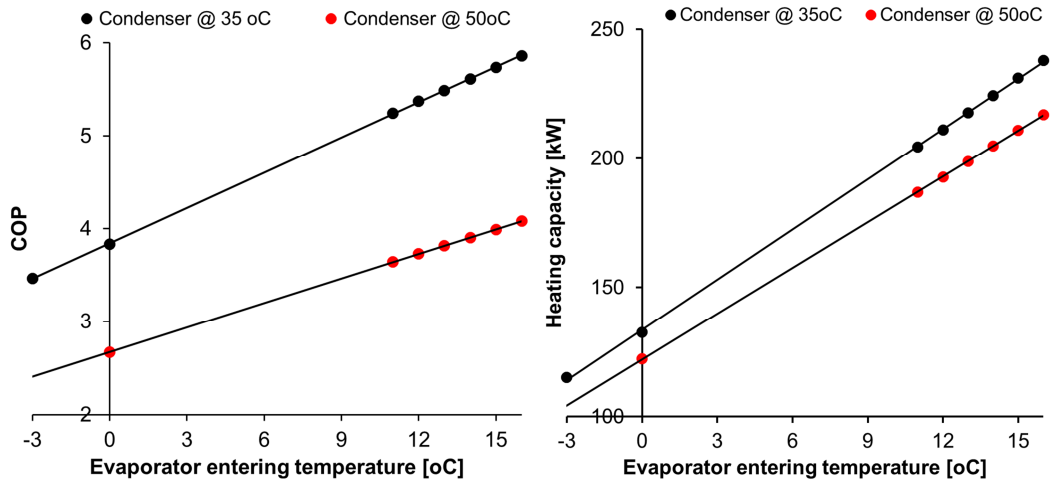
RECS-W 1902
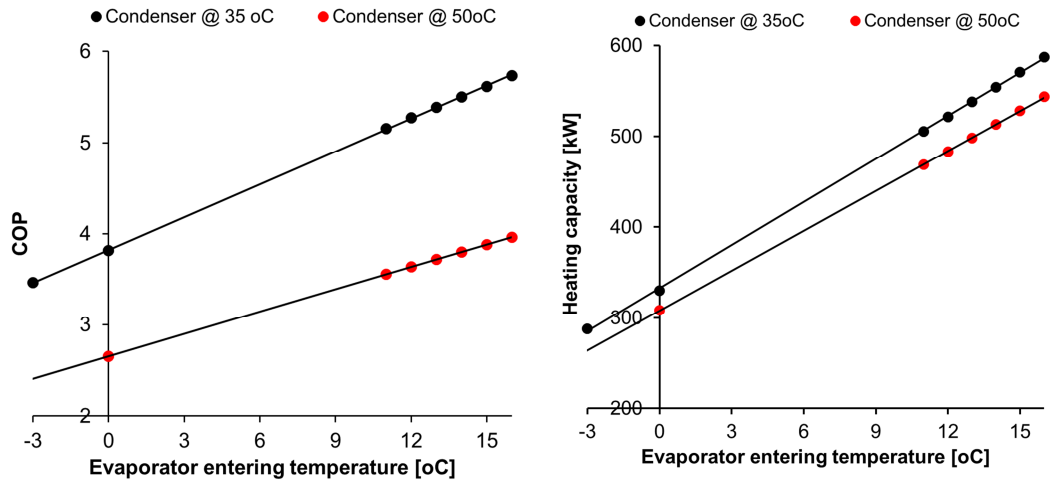
RECS-W 3202
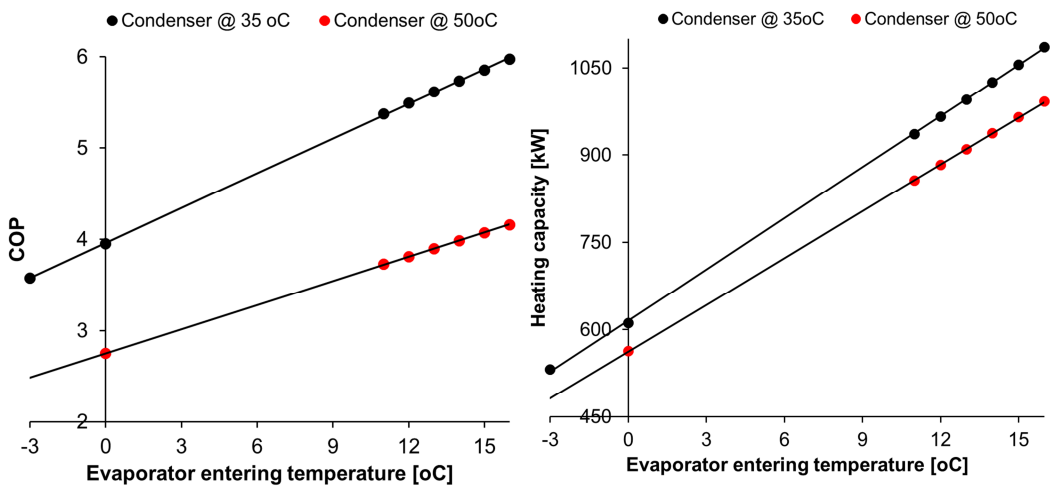
Figure 3.12: Performance of RECS-W heat pumps

52

4 Results

The results obtained from modelling of the reservoir and heat pump system will now be discussed. This will begin with a comparison of the results of the reservoir model with a previous model and experimental measurements. It will then continue with some general comments regarding the temperature variation observed in the reservoir during the year. Finally, the results of an open- and closed-loop heat pump scheme will be presented.

4.1 Thermal reservoir model

4.1.1 Validation

Results of a one year simulation are shown in Figure 4.1, alongside results from the model created by Chiasson, et al. (2000) and implemented in the TRNSYS environment.
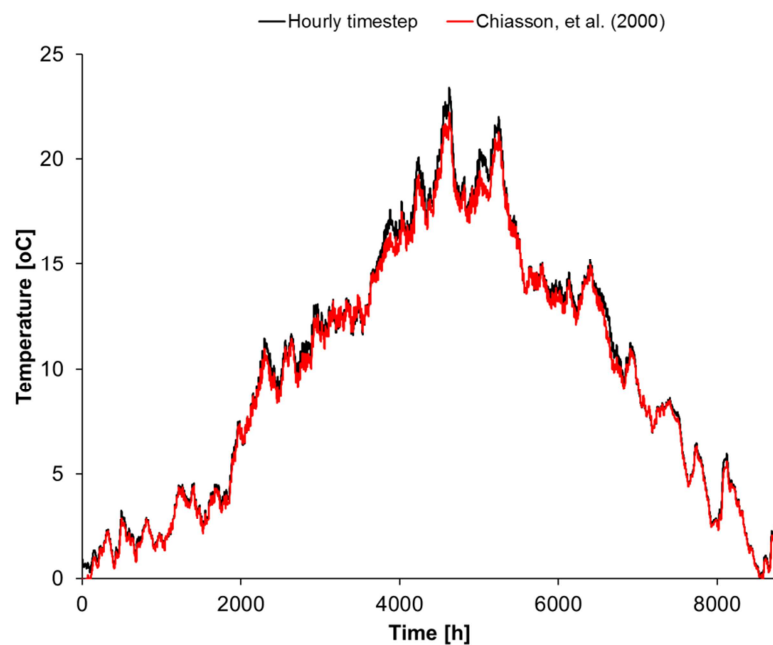
Figure 4.1: Annual reservoir temperature using hourly timestep and monthly energy balance models. Also shown is data taken from the model of Chiasson et al. (2000) implemented in TRNSYS

The general match between the predictions of the hourly timestep model and the Chiasson, et al. model shows good agreement, with small variations at a number of points. The most significant of these occurs at the start of the year when reservoir temperatures are at an annual minimum. This is believed to be caused by the conditions used to initiate the simulation, which differ slightly between the two models, and thus can be neglected. Over the course of a one year simulation, the average difference in the reservoir temperature predicted by the two models is low, at ~0.30^{o}C. The maximum difference in temperature is also relatively small at ~1.44^{o}C. Since the model developed by Chiasson, et al., has been validated previously, this may serve as a basic means against which to validate the thermal reservoir model. In the absence of experimental data for the annual reservoir temperature, this comparison with an already validated model seems a reasonable alternative.

Measurements of the reservoir temperature were made at ~15.00 August 1 by research staff at the University of St Andrews. Depth measurements were performed at approximately half and full depth in addition to at the water surface. Figure 4.2 shows all data points collected and Table 4.1 summarises the averaged results

Figure 4.2: Temperature-depth measurements at the centre of the Guardbridge Mill Loch
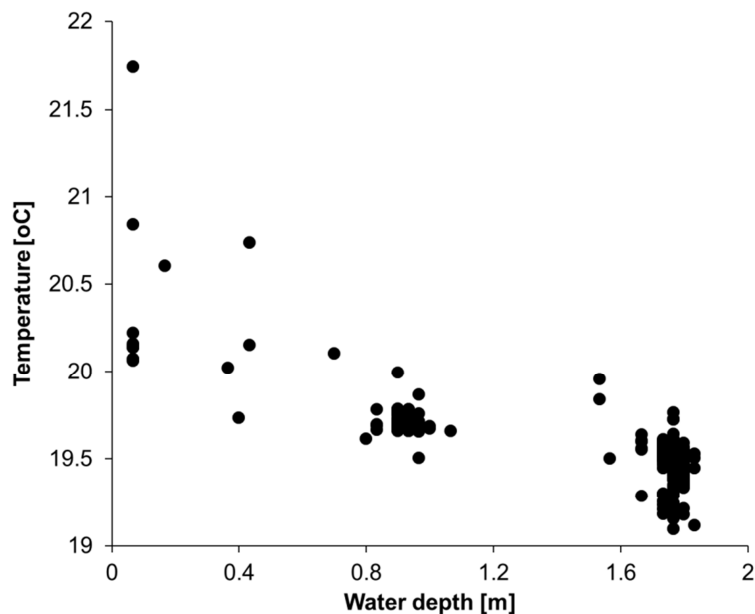
Depth [m]	Average temperature [^{o}C]
0	20.35
0.93	19.70
1.77	19.47

Table 4.1: Summary of temperature-depth measurements

Comparing these results with those obtained from the model, the model predicts a slightly lower temperature of 18.40^{o}C, compared to an average temperature of 19.84^{o}C as measured. However, since the model is based on "typical" annual weather data, a small variation from the measured results is not unexpected. Notably, higher than average solar radiation intensities in the weeks previous to the temperature-depth measurements in the reservoir are likely to have caused a higher than average temperature for this time of year. However, this could not be confirmed due to the absence of climate data for the period in question.

A second point to note is the thermal stratification that is shown to exist in the reservoir. This of the order of 1 - 2 K difference between the top and bottom surfaces. This can be considered to be fairly small considering uncertainties in both the measurement equipment and in the mathematical model, and thus does not invalidate the lumped capacitance approach adopted in the model.

4.1.2   Reservoir temperature trends

With reference to Figure 4.3, the general trend in the reservoir temperature over the year is clearly defined. Over the first three months of the year there is a gradual increasing trend, which then increases significantly over a shorter time period, and then returns to a more gradual increase in temperature. Peak temperatures occur in July, with a maximum temperature of 23.43K. Significant variation is observed according to climatic conditions, with air temperature and solar radiation incident on the reservoir the two climatic factors with greatest influence over the reservoir temperature. Figure 4.4 shows the trends of the reservoir temperature alongside the ambient dry bulb temperature and the monthly average daily solar insolation. The

sudden rise in reservoir temperature near the beginning of spring (~2000 h) can be seen to be related to an increase in the ambient air temperature during this period.
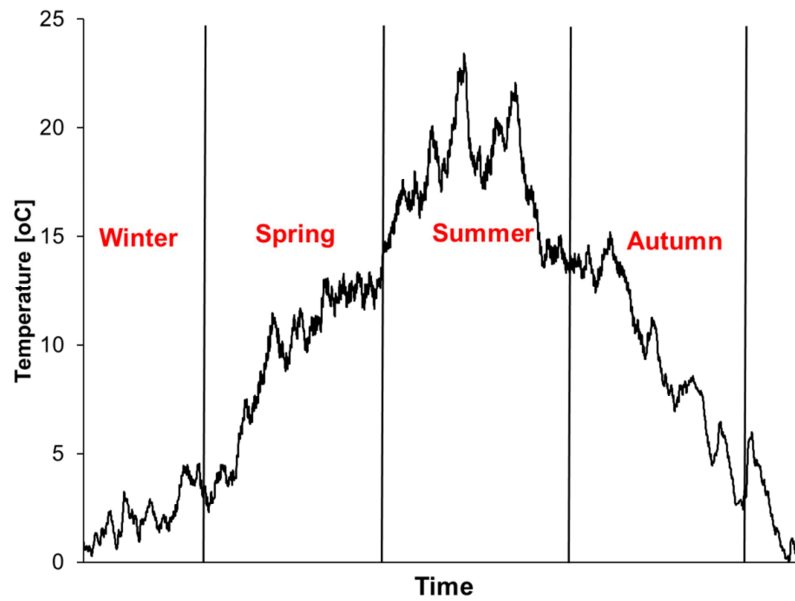
Figure 4.3: Guardbridge Mill Loch temperature variation over a year
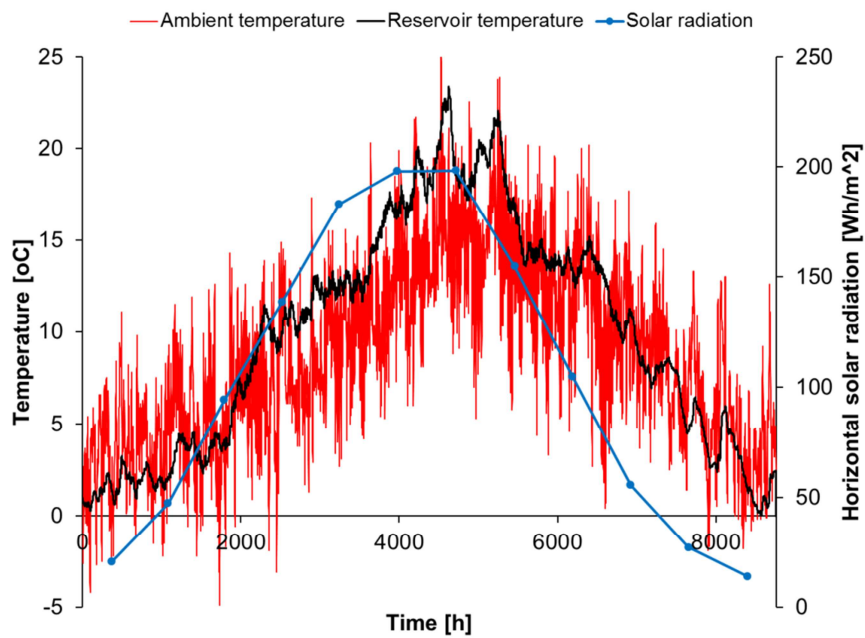
Figure 4.4: Influence of ambient temperature and solar insolation on reservoir temperature

An indication of the relative importance of the four heat transfer mechanisms in the model is shown in Figure 4.5. Heat loss by thermal radiation is shown to be fairly constant throughout the year, while evaporative losses become greater in the summer when the greater difference in temperature between the reservoir and the air drives the process. Similarly, the sensible heat transfer between the two bodies is greater in the warmer months for the same reason. Clearly the solar radiation absorbed by the reservoir is very significant in the overall temperature across the year, and is the most significant means of heat transfer. In the winter period, it can be seen that the heat transfer to the pond is much smaller and more closely matches that lost by evaporation. Therefore it is during this period that the reservoir will be much more sensitive to temperature changes which a heat pump will introduce.
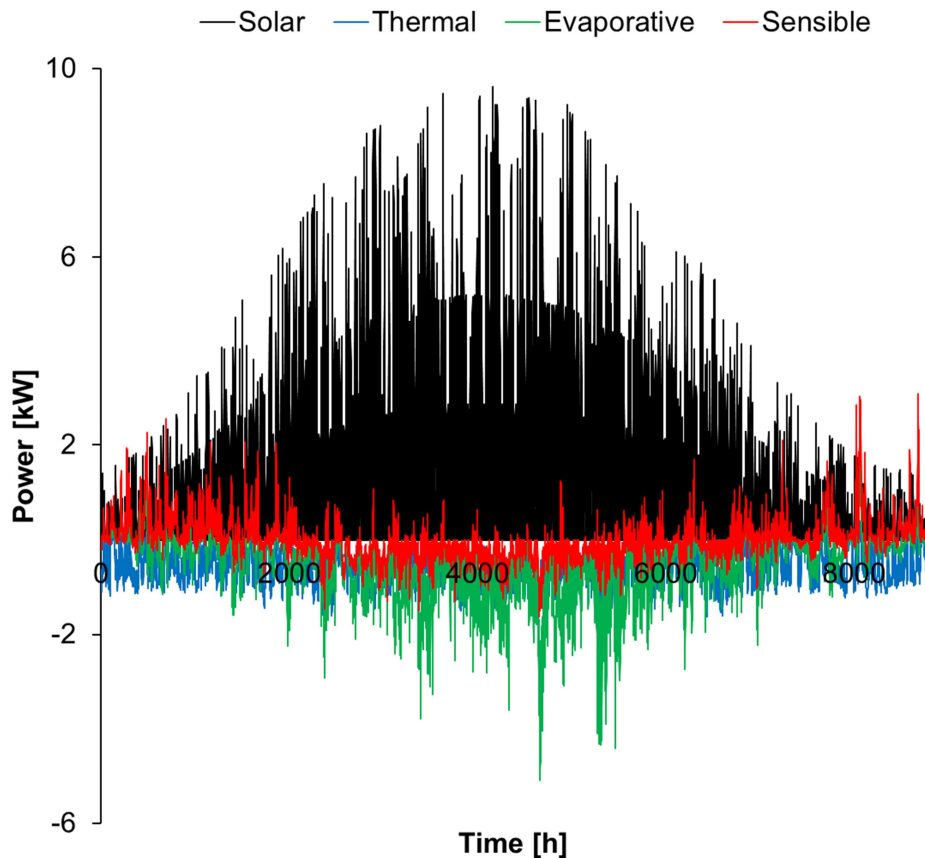
Figure 4.5: Heat transfer in and out of reservoir by various mechanisms across a year

One thing that is clear from the model is that the reservoir is highly responsive to changes in environmental conditions, and the temperature can vary be several degrees in a 24h period. Thus the performance of any heat pump will be highly variable on this short timescale, in addition to much larger fluctuations on a longer time basis.

4.1.3 Open-loop scheme

An open-loop scheme could extract water from the reservoir by pipe and transport this to the main heat pump unit(s). As was discussed in section 3.1, there is an existing 18 inch pipe which takes water from the reservoir into the main Guardbridge site via the filter house, which could potentially be used for this purpose. Additionally there is a 14 inch pipe which can take water directly from the mill lade upstream and bypass the reservoir, feeding directly into the filter house. Since an open loop scheme would take water directly from the reservoir, it would be necessary refill the reservoir to compensate this water loss. The modelling performed has been based on maintaining a constant water level at all times, though in actuality the water level may be maintained at a higher or lower level as desired.
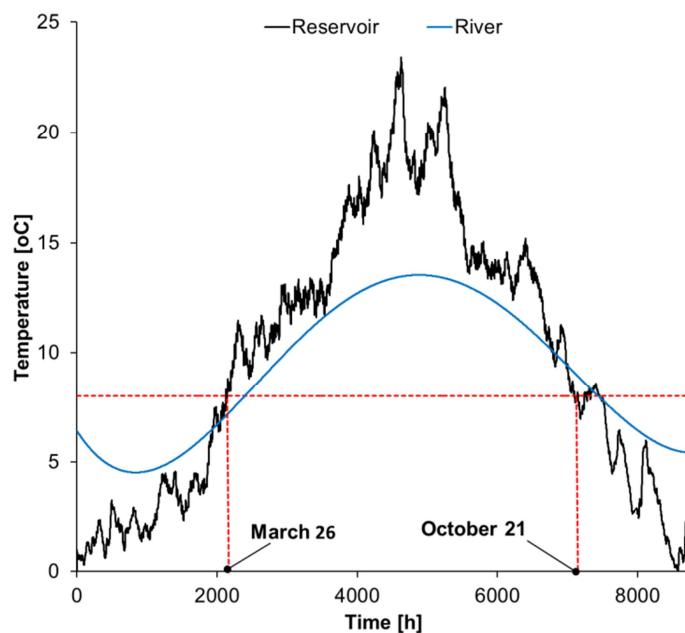
Figure 4.6: Reservoir temperature in relation to minimum operating temperature for an open loop heat pump scheme

58

Figure 4.6 illustrates the reservoir temperatures over a typical year in relation to the minimum operating condition of an open loop heat pump scheme. The manufacturer's quoted minimum evaporator entering fluid temperature is 8°C, which means that for an open loop scheme using the reservoir water directly, any heat pump will only be operable at reservoir temperatures above this temperature. This limit is also advised by other sources (YouGen, 2012), which note that this is put in place to prevent problems with ice formation on the evaporator heat exchanger. Maximum evaporator inlet temperature for the heat pump is quoted at 23°C which should not present a problem given the annual temperature trend of the reservoir, which has a maximum value of $\sim23.4^{\circ}$C. Cold water could also be mixed with the reservoir supply water if temperatures were to exceed this upper value.

Taking this into account, the simulation results suggest that an open loop scheme would be unable to operate in the weather conditions experienced at Guardbridge for a significant part of the year, approximately 6 months. During this time reservoir temperatures are predicted to be below the minimum 8°C threshold for safe operation.

Similarly, the temperatures which could be expected in the Motray water are also unlikely to meet the minimum threshold for a similar proportion of the year, ruling this out as an alternative heat source for an open loop scheme. It can therefore be concluded that an open loop scheme would likely be operable only during the best part of the spring and autumn, and the summer months, assuming that antifreeze cannot be added to the water due to environmental reasons.

The likely performance of an open loop scheme during these warmer periods will now be discussed. Simulations were performed for RECS-W 0802, 1902 and 3202 models, at condensing water output temperatures of 35°C and 50°C. Reservoir flow rates were as described in section 3.1 and COP and heating capacity values were calculated using the relations given in Table 3.1. The results for the RECS-W 0802 model are shown in Figure 4.7, for 1902 in Figure 4.8 and for 3202 in Figure 4.9.

59
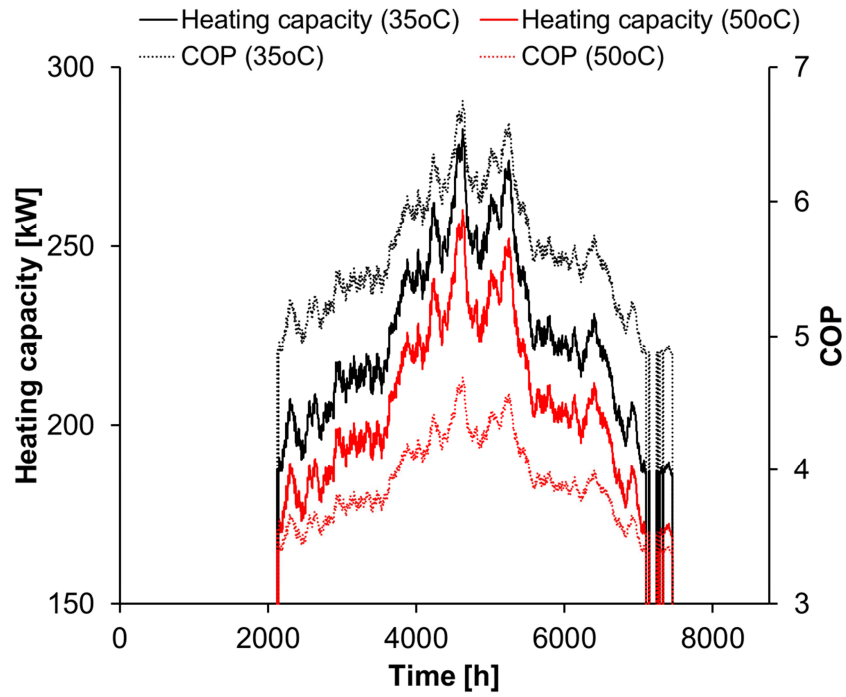
Figure 4.7: Performance of RECS-W 0802 heat pump in open loop scheme
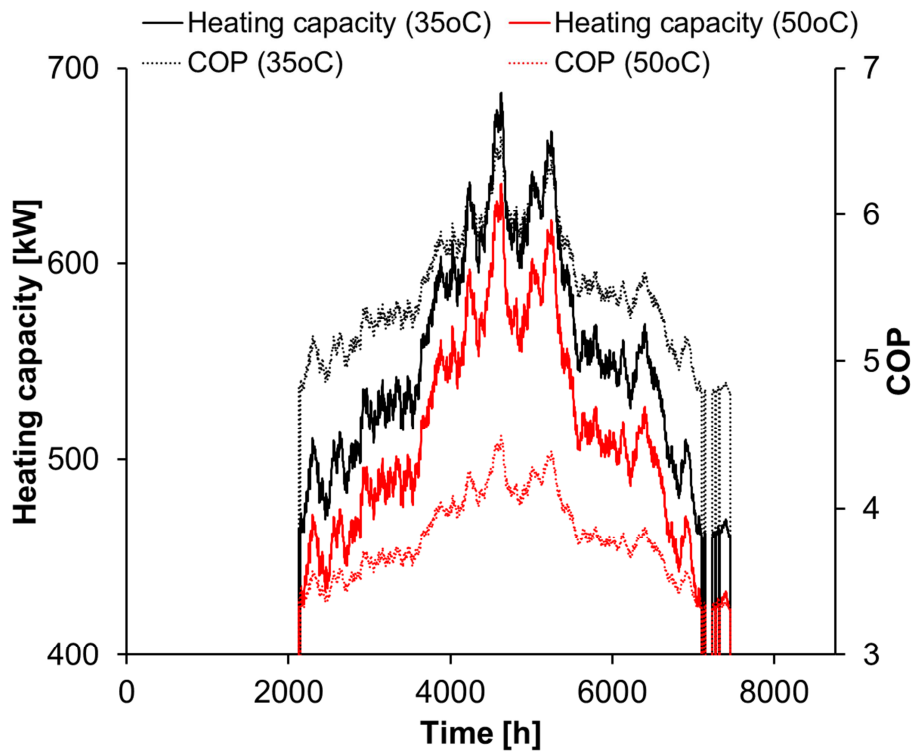
Figure 4.8: Performance of RECS-W 1902 heat pump in open loop scheme
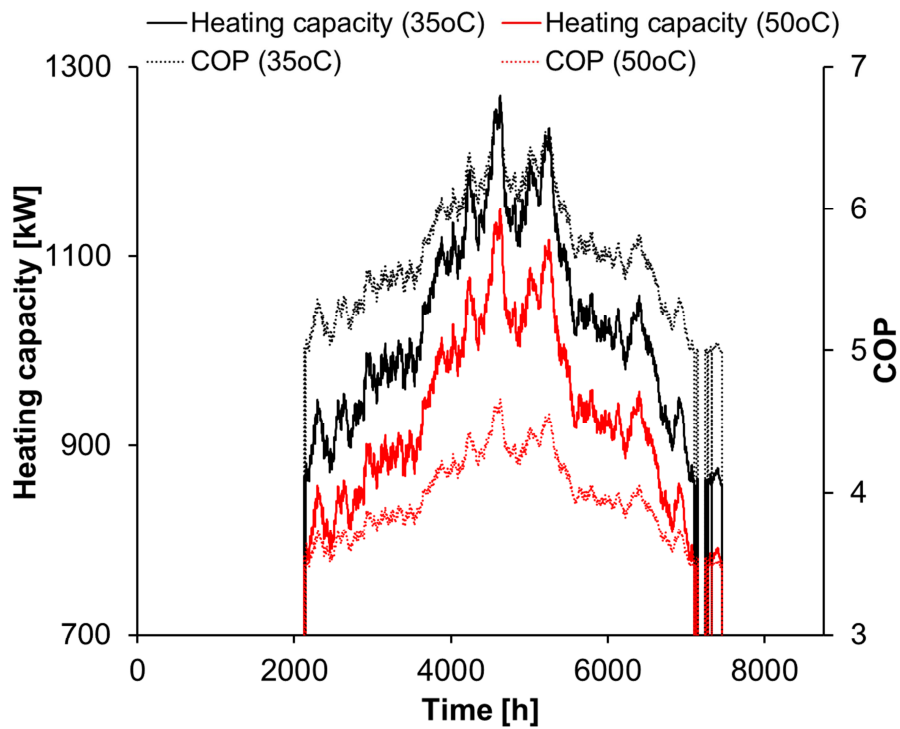
Figure 4.9: Performance of RECS-W 3202 heat pump in open loop scheme

Neglecting those periods during which the heat pumps are incapable of operation due to low temperatures, the COPs may be as high as 6.75 at maximum, and around 3.31 at the lowest simulated value. The results are summarised in Table 4.2.

Heat pump model	Condenser output temperature [oC]	COP			Heating capacity [kW]		
		Max.	Min.	Avg.	Max.	Min.	Avg.
0802	35	6.75	4.86	5.62	283	186	225
	50	4.69	3.38	3.91	260	169	206
1902	35	6.53	4.79	5.50	688	460	553
	50	4.49	3.31	3.79	641	423	512
3202	35	6.72	4.98	5.70	1270	857	1027
	50	4.66	3.47	3.96	1150	774	929

Table 4.2: Summary of results for open loop heat pump scheme

The results suggest that an open loop scheme could provide substantive heating capacity, and high COPs, according to the time of year, and the exact nature of the system adopted. It is clear that a lower water output temperature of 35°C gives a higher COP and higher heating capacity, and should therefore be adopted if at all possible over a higher temperature output. It should also be noted that the heat pump model with the lower heating capacity gives slightly higher COPs than the larger unit. This may suggest that using several smaller units over a single unit with a larger capacity may be marginally beneficial in terms of the COP achieved, although other considerations would need to be considered, such as additional piping required and space considerations. Additionally, when the higher flow rate required for additional small units is taken into account, the overall reservoir temperature is be lower which results in a small decrease in performance.

Generally, it can be seen that due to the high flow rates permitted in the system due to the high volume of water in the reservoir and the large pipe already in place, a heat pump with a significant capacity could readily operate on this flow with good COPs. However, the fact remains that an open-loop scheme would only be operable for around half of the year, mainly during warmer weather when heating demand is likely to be lower. The merits of such a scheme are therefore highly questionable.

Any water abstracted from the reservoir for use in an open loop system would normally be returned to the Motray Water from which it was originally taken. Legislation regarding the management of fresh water habitats is required by the European Union Fresh Water Fish Directive (Directive 2006/EE/EC), and enforced in Scotland through the Surface Waters (Fishlife) (Classification) (Scotland) Regulations 1997. These regulations define limits on the temperature variation permitted in rivers due to thermal discharge according to two classifications, salmonid and cyprinid waters, of which the Motray Water is a salmonid water (SEPA, 2007). The legislation states that at the edge of the mixing zone downstream of a thermal discharge, the temperature must not exceed 1.5^{o}C of the unaffected temperature, and the temperature must not exceed 21.5^{o}C. However, there do not appear to be similar stipulations for the case of heat extraction from a water body.

Consideration must also be given to the water quality, in particular the water pH. Water with a lower pH (acidic) will results in problems with corrosion of pipes and the heat exchanger, requiring corrosion resistant equipment to be used. Similarly water with a high pH may cause scaling. The Baylis curve in Figure 4.10 shows the range of pH and alkalinity in which water can be considered stable. Alkalinity is measured in parts per million of calcium carbonate ($CaCO_3$).
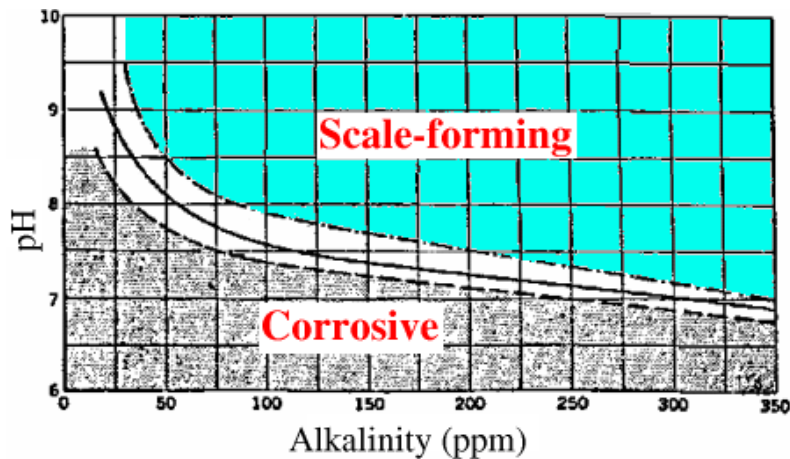
Figure 4.10: The Baylis curve which indicates required water pH and alkalinity for stable water (Mountain Empire Community College, n.d.)

Consideration must also be given to the energy required to pump the water from the reservoir to the heat pump unit. As mentioned in section 2.1.2, the COP does not take into account additional energy costs associated with pumping water from the reservoir to the heat pump and onwards to the Motray water. Therefore more detailed system design and pumping energy costs would need to be performed in order to fully understand the energy economics of such a scheme.

4.1.4 Closed-loop scheme

A closed loop scheme would operate by placing a series of heat exchangers in the reservoir, through which an anti-freeze solution is passed, collecting heat from the water, before carrying this to the evaporator of the heat pump unit. This type of system has the advantage that the anti-freeze can be reduced to temperatures less than $0^{o}C$ and remain as a liquid, thus allowing heat transfer at lower temperatures than

water alone. In the case of the Guardbridge site, this could take one of two basic forms, a normal or split system, as elaborated in section 2.2.3 (see also). Note that in the modelling performed, heat losses for either the anti-freeze or refrigerant solutions are not considered, and therefore neither system is specifically modelled. However, it is the understanding of the author that a conventional system where the evaporator and condenser are located together is normal practice.

In order to maximise the temperatures in the reservoir, and thereby achieve the highest possible performance from a closed-loop system, water from the Motray water should be used to replace the reservoir water when temperatures in the Motray are higher than those predicted in the reservoir. Returning to Figure 4.6, it is observed that it will be beneficial to replace reservoir water with lade water during approximately the first 3 and last 2 months of the year. All simulations assume this behaviour. Simulations were performed using various heat exchanger areas and heat pump models, assuming 30% glycol solution as the transfer fluid. The results are shown in for the three models are shown in Figure 4.11, Figure 4.12 and Figure 4.13 .
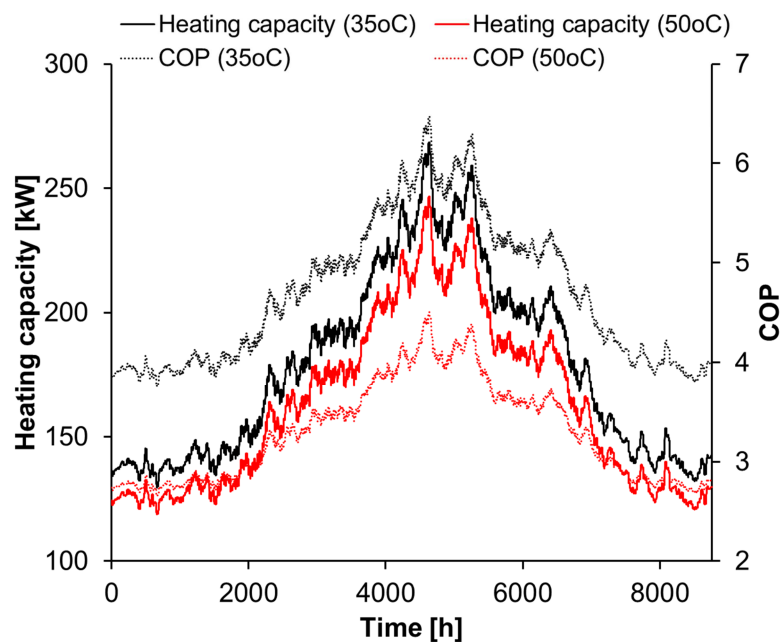
Figure 4.11: Performance of RECS-W 0802 in closed loop scheme
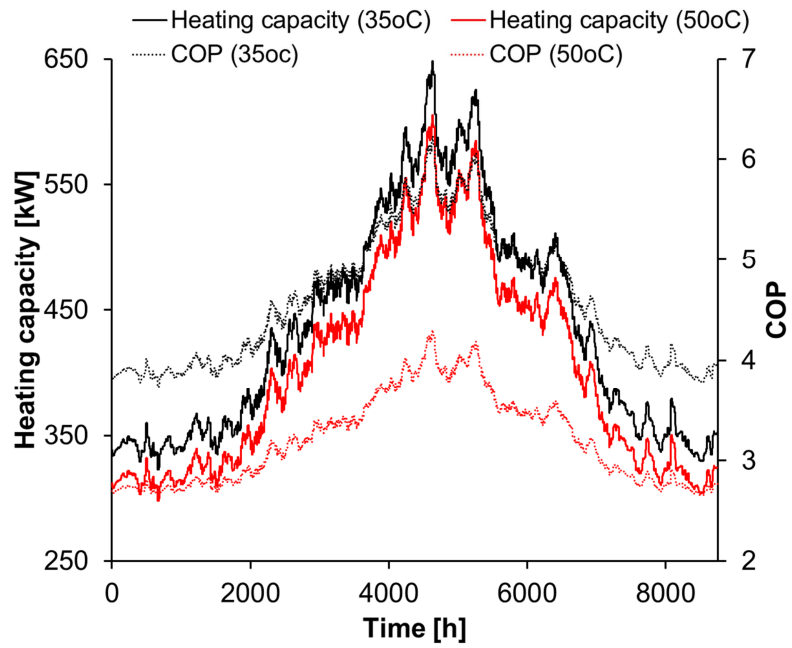
Figure 4.12: Performance of RECS-W 1902 in close loop scheme
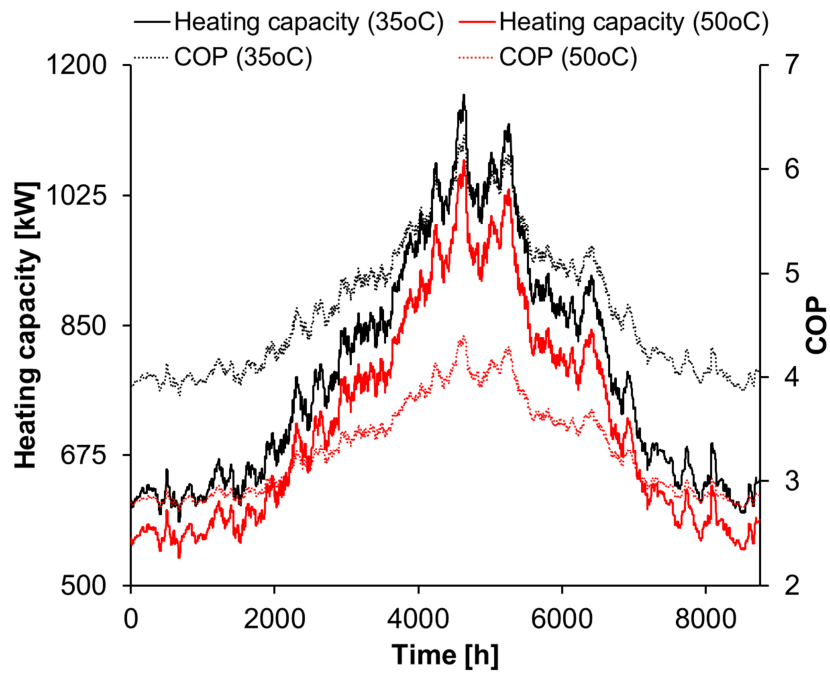
Figure 4.13: Performance of RECS-W 3202 heat pump in closed loop scheme

65

The results are also summarised in Table 4.3. The total heat exchanger area used for each model of heat pump was as shown in Table 4.4. These exchanger areas were selected on the basis of experimentation which showed that this was the minimum exchanger area required to maintain an evaporator entering temperature of greater than 0°C, which was given by the manufacturer as the minimum condition for an output of 50°C (Young, 2013).

Heat pump model	Condenser output temperature [oC]	COP			Heating capacity [kW]		
		Max.	Min.	Avg.	Max.	Min.	Avg.
0802	35	6.48	3.76	4.71	268	130	179
	50	4.51	2.66	3.30	247	119	163
1902	35	6.23	3.74	4.60	648	323	436
	50	4.30	2.63	3.21	606	298	405
3202	35	6.32	3.83	4.69	1160	586	786
	50	4.41	2.72	3.31	1071	539	723

Table 4.3: Summary of results for closed loop heat pump scheme

Heat pump model	Heat exchanger area [m^2]	Approximate number of SJ-10T plates
0802	100	9
1902	250	23
3202	450	41

Table 4.4: Heat exchanger areas used in simulations

The results indicate that a closed loop heat pump scheme could successfully operate in the reservoir, with the potential for high heating capacity with a maximum capacity of 1160kW using a single RECS-W 3202 heat pump with around 41 heat Slim Jim plates, if an output of 35°C was selected. Due to the significant temperature variation in the reservoir over the year, there is consequently a significant range of heating capacities and COPs according to the season, with a total range of approximately 550

kW for the largest heat pump model. Therefore, although the RECS-W 3202 has a quoted heating capacity of 860 kW, it could only reliably support a maximum load of closer to 500 kW when used at the sources temperatures in this situation. It should also be noted that in the winter season, when heating demand is likely to be highest, that the COPs achieved are fairly low, with a minimum of around 2.72 for the 3202, and even lower for smaller capacity units.

In considering the possibility of a larger capacity system, multiple pumps may be used with separate heat exchanger circuits. For example Figure 4.14, shows the expected performance from 2 RECS-W 3202 heat pump units operating with independent heat exchanger circuits in the reservoir, each with 550 m^2 of heat exchanger area. Due to the large volume of water contained in the reservoir, a large amount of heat can be removed before any serious drop in performance can be expected. However, it should be noted that a significant heat exchanger area would need to be implemented, perhaps around 1100 m^2, equivalent to approximately 100 SJ-10T flat plate heat exchanger panels.
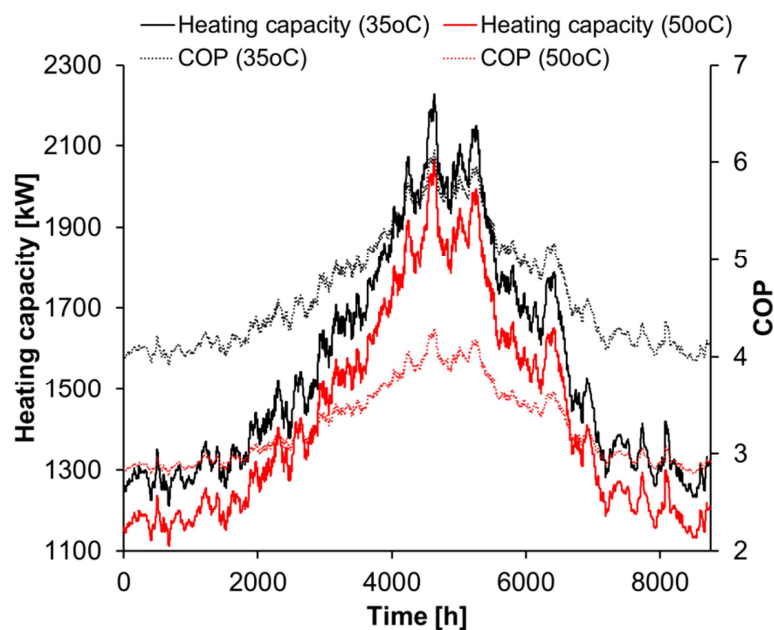
Figure 4.14: Performance of two RECS-W 3202 heat pumps in a closed loop scheme

The main limiting factors in the size of heat pump system which would be introduced are namely then the heat exchanger surface area required to support the system. However if we assumed that the reservoir surface area of 11,500 m^2 is equal to the reservoir floor on which heat exchangers may be placed, and each plate has a footprint of ~0.38 m^2 (AWEBGEO, 2013), it is observed that only around 0.3% of the reservoir floor would be required to house plates in order to house 100 plates.

An additional issue which has not been considered in the modelling performed is that of ice formation on the surface of heat exchanger plates. Since the glycol fluid in the heat exchanger is at times below 0°C, a layer of ice is likely to form on the plate surface due to the transfer of heat from the reservoir water to the glycol. Figure 4.15 shows the change in the reservoir temperature, and of the glycol entering and leaving the heat exchanger system for a single RECS-W 3202 pump with an output of 35°C, for various total heat exchanger areas. It is clear that a larger total heat exchanger area will reduce the risk of ice formation on the plates, since the average temperature of the glycol will be greater. Additionally, any frost would be spread over a greater area which would reduce the overall reduction in heat transfer. However, greater modelling would need to be performed in order to better understand the effects of ice formation on the heat exchangers.

Additionally a greater heat exchanger area is shown to results in more efficient overall performance due to greater heat transfer to the glycol solution and hence a higher evaporator temperature (see Figure 4.16). The results, summarised in Table 4.5 show that a significant improvement in performance can be obtained by increasing the heat exchanger area beyond the minimum required for heat pump operation. For instance, taking the 3202 model as an example, increasing the heat exchanger area by 150 m^2 from 450 to 600 m^2 gives an additional minimum heating capacity of 45 kW, and increases the average COP by 0.18. This is equivalent to adding approximately 14 additional heat exchanger panels.

Heat exchanger area [m^2]	COP			Heating capacity [kW]		
	Max.	Min.	Avg.	Max.	Min.	Avg.
450	6.32	3.83	4.69	1160	586	786
600	6.50	4.02	4.87	1201	631	827
850	6.67	4.21	5.05	1240	675	868

Table 4.5: Summary of investigation in the effect of heat exchanger area on performance

In the preceding section, results obtained from mathematical modelling were presented. This included a comparison of model results with those of an existing model and experimentally obtained data. Some discussion of the annual temperature profile of the reservoir was discussed and results were given for open- and closed-loop heat pump schemes. The report will now conclude with a summary of the main results obtained in the work and some suggestions for further work to be performed.
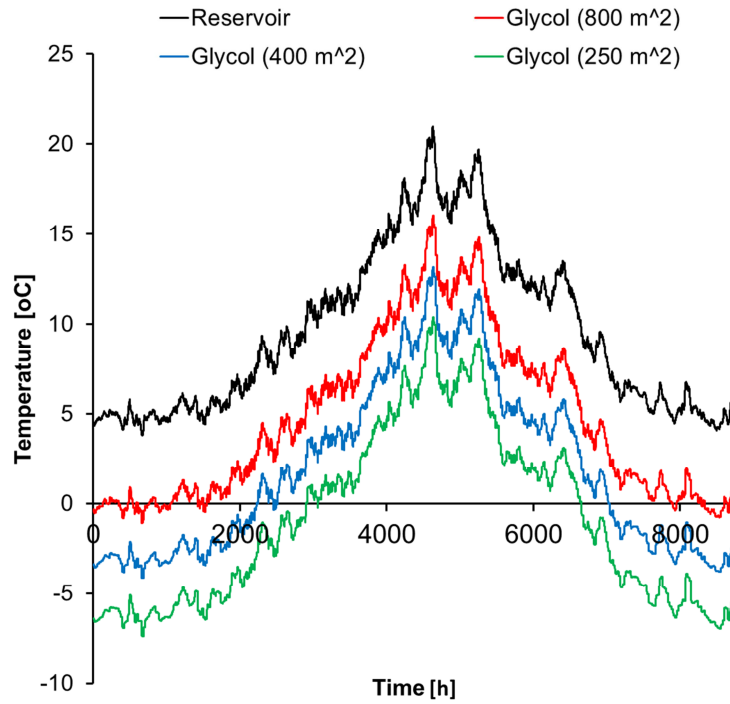
Figure 4.15: Reservoir temperature and average glycol temperature for RECS-W 3202 heat pump with various heat exchanger areas
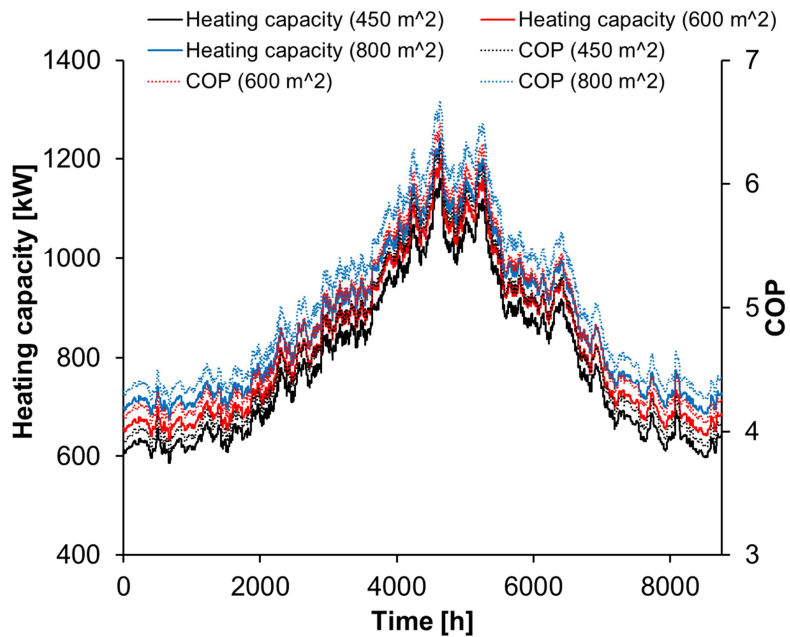
Figure 4.16: Relation between RECS-W 3202 (35°C condenser) heat pump performance and heat exchanger area

5 Conclusions

In this project, an investigation was performed into the potential to develop a WSHP scheme using a freshwater reservoir by the use of a mathematical model.

A mathematical model of a reservoir was developed in the Freemat environment using a combination of first principles and empirical calculations for heat transfer including solar gains, thermal radiation, sensible transfer, evaporative losses and the addition of water. Using local climatic data, this was validated both against an existing model and with experimental measurements of the real reservoir temperature at a single point in time. The model predicts annual minimum temperatures of a few degrees and maxima of around 23°C.

Empirical relations were developed using manufacturer's performance data to assess the performance of a range of WSHP models, at various evaporator temperatures. These empirical relations were then used in combination with the mathematical model to predict the performance of various heat pump schemes. The results indicate that an open loop scheme would be largely unsuitable due to the low water temperatures in the reservoir during the colder months, despite potentially high heating capacities of over 1 MW possible due to the high flow rate and temperatures in the warmer months. Similarly high COPs of around 4 or 5 depending on the temperature output, either 35°C or 50°C. It was also concluded that the flow rate available from the reservoir is sufficient to support multiple heat pumps in order to increase overall heating capacity. It is also possible than the period of operation could be extended by increasing the water flow rate during cold periods, which would allow similar heat extraction overall but with a lower temperature drop in the water. However, this was not covered in the project and could be looked at in more detail as further work.

In terms of a closed-loop scheme, it was shown that this would be able to operate year round using an additional glycol loop in the reservoir and Slim Jim flat plate heat exchangers. Modelling showed that the reservoir could potentially support multiple heat pumps, supporting a heating load of over 1 MW with COPs of 3-4 at an output of

71

50°C and 5-6 at 35°C. The advantage of a greater number of heat exchanger plates was also illustrated, with significant improvements in heating capacity and COP achievable by increasing total heat exchange area.

However, further work should be performed in order to confirm the viability of a closed-loop scheme. This would include further research into the effect of ice formation on heat exchanger plates during cold weather, which it is suspected will reduce overall performance due to a reduction in the heat transfer coefficient between the reservoir water and the plates. Investigation could also be performed into the relative benefits of flat plate exchangers over conventional HDPE loops, which were not considered in this project. Greater consideration must also be given to the associated costs of any scheme, particularly the merits over other potential options such as air-source heating or a ground-source scheme.

In should also be noted that in any forthcoming project, the normal process adopted would be to determine the maximum heating load expected, determine the lowest reservoir temperature experienced, and select a system capable of producing the maximum load at this minimum evaporator temperature.

6 Appendixes

6.1 Reservoir open-loop heat pump model

```
%Load climate file
climate_file=csvread('leuchars_climate.csv',1,0); %For column definitions see file

%Create water top up schedule
fill=(61.1/3600);

%Create heat pump schedule
hp_schedule=[0,0,0,0,0,0,1,1,1,1,1,1,1,1,1,1,1,1,0,0,0,0,0,0];
heat_pump_profile=repmat(transpose(hp_schedule),365,1);

%Set initial and final timesteps
tstart=1;               %Set initial time
t=tstart;               %Set initial time
no_years=1;             %Set the number of years to run for
tend=8760*no_years;   %Set end time

%Create empty matrix for results files
temperature_results=zeros([tend,3]);     %Create reservoir temperature results table
energy_results=zeros([tend,4]);          %Create heat transfer results table

%Define reservoir geometry
reservoir_area=11500;       %Define reservoir area [m^2]
reservoir_volume=30927;     %Define reservoir volume [m^3]
reservoir_depth=2;          %Define reservoir depth [m]

%Define reservoir parameters
extinct=10;         %Define water extinction coefficient
emissivity=0.96;    %Define water emissivity
nair=1;             %Define air refraction index
nwater=1.33;        %Define water refraction index

%Set initial values
reservoir_temp=climate_file(tstart,1);   %Set initial reservoir temperature
Q_solar=0;                               %Set initial solar radiation heat transfer
Q_thermal=0;                             %Set initial thermal radiation heat transfer
Q_sens=0;                                %Set initial sensible heat transfer
Q_evap=0;                                %Set initial evaporative heat transfer

%%%%%%%%%%%%%%%%%%%%%%%%%%%%%%%%%%%%%%%

%Begin timestep
```

while t<tend

%Load climate data
dry_bulb=climate_file(t,1);   %Set dry bulb temperature [oC]
dew_point=climate_file(t,2);   %Set dew point temperature [oC]
relative_humidity=climate_file(t,3);   %Set relative humidity [%]
solar_intensity=climate_file(t,4);   %Set gloal horizontal radiation intensity [W/m^2]
wind_speed=climate_file(t,5);   %Set wind speed [m/s]
sky_temp=climate_file(t,6);   %Set effective sky temperature [K]
solar_incident_angle=climate_file(t,8);   %Set solar incident angle [o]
atmospheric_pressure=climate_file(t,10);   %Set atmospheric pressure [Pa]
river_temp=climate_file(t,12);   %Set river water temperature [oC]

%%%%%%%%%%%%%%%%%%%%%%%%%%%%%%%%%%%%%%

%Calculate solar radiation heat transfer
solar_incident_rad=solar_incident_angle*pi/180;   %Convert incident angle to radians
refract=asin(sin(solar_incident_rad)*nair/nwater)+0. %Calculate angle of refraction
rperp=(sin(refract-solar_incident_rad))^2/(sin(refract+solar_incident_rad))^2;
%Calculate perpendicular component of reflection
rpara=(tan(refract-solar_incident_rad))^2/(tan(refract+solar_incident_rad))^2;
%Calculate parallel component of reflection
TAOr=0.5*((1-rperp)/(1+rperp)+(1-rpara)/(1+rpara)); %Calculate transmittance of reservoir surface
TAOa=exp(-1*extinct*reservoir_depth/cos(refract)); %Calculate absorbance of reservoir surface
reflectivity=TAOa-TAOa*TAOr;   %Calculate reflectivity of reservoir surface
Q_solar=solar_intensity*(1-reflectivity)*reservoir_area; %Calculate solar radiation heat gain [W]

%Calculate thermal radiation heat transfer
Q_thermal=reservoir_area*emissivity*(5.67E-8)*((reservoir_temp+273)^4-(sky_temp^4)); %[W]

%Calculate evaporative heat transfer
e0=610.8*exp((17.27*reservoir_temp)/(237.7+reservoir_temp)); %Calculate saturation vapour
pressure [Pa]
ea=610.8*exp((17.27*dew_point)/(237.7+dew_point));   %Calculate actual vapour pressure [Pa]
evaprate=0.000968*wind_speed*(e0-ea);   %Calculate water evaporation rate
[mm/day]
Q_evap=(2.45*1*evaprate*reservoir_area*1000)/86.4;   %Calculate evaporative heat transfer [W]

%Calculate sensible heat transfer
Q_sens=Q_evap*66*(dry_bulb-reservoir_temp)/(e0-ea); %[W]

%Calculate energy transfer by addition and removal of water
if reservoir_temp>8 & heat_pump_profile(t,1)==1
   Q_water=fill*density_water(river_temp)*water_cp(river_temp)*(river_temp-reservoir_temp);
   water=fill;
else

74

```matlab
    Q_water=0;
    water=0;
end

%Calculate total energy flow and net energy flow
Q_in=Q_solar+Q_sens+Q_water;        %Calculate heat gain [W]
Q_out=Q_thermal+Q_evap;             %Calculate heat loss [W]
Q_net=Q_in-Q_out;                   %Calculate net energy transfer [W]

%Define reservoir properties
reservoir_cp=water_cp(reservoir_temp);          %Calculate pond cp
reservoir_rho=density_water(reservoir_temp);    %Calculate pond density

%Calculate temperature change and new reservoir temperature
delta_T=(Q_net*3600)/(reservoir_cp*reservoir_volume*reservoir_rho);    %Calculate delta T for
timestep [K]
reservoir_temp=real(reservoir_temp+delta_T); %Calculate new reservoir temperature [oC]

%%%%%%%%%%%%%%%%%%%%%%%%%%%%%%%%%%%%%

%Save results to matrix
temperature_results(t,1)=reservoir_temp;
temperature_results(t,2)=water;
energy_results(t,1)=Q_solar;
energy_results(t,2)=Q_sens;
energy_results(t,3)=Q_thermal;
energy_results(t,4)=Q_evap;
energy_results(t,5)=Q_in;
energy_results(t,6)=Q_out;
%Set time for next timestep
t=t+1;
end

%%%%%%%%%%%%%%%%%%%%%%%%%%%%%%%%%%%%%
%Save model results to .csv file
plot(temperature_results(:,1))                   %Plot temperature of reservoir
xlim([tstart,tend])
csvwrite('main_results.csv',temperature_results)   %Write main results to .csv file
csvwrite('energy_results.csv',energy_results)      %Write enegy transfer results to .csv file
```

6.2 Reservoir closed-loop heat pump model

```
%Set initial and final timesteps
tstart=1;                   %Set initial time
t=tstart;                   %Set initial time
no_years=2;                 %Set the number of years to run for
tend=8760*no_years;   %Set end time

%Load climate file
climate_file=csvread('leuchars_climate.csv',1,0); %For column definitions see file

%Load river flow rate file
river_flow_file=csvread('Motray_water_flow.csv',1,0);

%Create water top up schedule
schedule=[1,1,1,1,1,1,1,1,1,1,1,1,1,1,1,1,1,1,1,1,1,1,1,1];
river_top_up=repmat(transpose(schedule),365*no_years,1);

%Create heat pump schedule
hp_schedule=[0,0,0,0,0,0,1,1,1,1,1,1,1,1,1,1,1,1,0,0,0,0,0,0];
heat_pump_profile=repmat(transpose(hp_schedule),365*no_years,1);

%Set conditions for iterative solution
limit=5000;                 %Set tolerance for heat transfer
temperature_step=0.005;  %Set increments for temperature guess

%Create empty matrix for results files
temperature_results=zeros([tend,3]);     %Create reservoir temperature results table
energy_results=zeros([tend,4]);          %Create heat transfer results table

%Define reservoir geometry
reservoir_area=11500;     %Define reservoir area [m^2]
reservoir_volume=30927; %Define reservoir volume [m^3]
reservoir_depth=2;         %Define reservoir depth [m]

%Define reservoir parameters
extinct=10;                 %Define water extinction coefficient
emissivity=0.96;          %Define water emissivity
nair=1;                     %Define air refraction index
nwater=1.33;               %Define water refraction index

%Define heat exchanger properties
exchanger_area=850;         %Define the heat exchanger area [m^2]
fluid_in=-6;                 %Set heat transfer fluid inlet temperature [oC]
fluid_out=fluid_in;          %Set heat transfer fluid outlet temeprature [oC]
char_length_x=1.2192;        %Define heat exchanger height [m]
```

```matlab
volumetric_flow_rate=114;    %Set transfer fluid mass flow rate [m^3/h]

%Set initial values
reservoir_temp=climate_file(tstart,1);      %Set initial reservoir temperature
Q_solar=0;                                  %Set initial solar radiation heat transfer
Q_thermal=0;                                %Set initial thermal radiation heat transfer
Q_sens=0;                                   %Set initial sensible heat transfer
Q_evap=0;                                   %Set initial evaporative heat transfer
Q_pump=0;                                   %Set initial heat pump capacity
fluid_average=real(fluid_in+fluid_out)/2;   %Set initial average glycol temperature
COP=3;                                      %Set initial heat pump COP
filmW_T=(reservoir_temp+fluid_average)/2; %Set initial film temperature

%%%%%%%%%%%%%%%%%%%%%%%%%%%%%%%%%%%%%%%%%%%%%

%Begin timestep
while t<tend
t
%Load climate data
dry_bulb=climate_file(t,1);             %Set dry bulb temperature [oC]
dew_point=climate_file(t,2);            %Set dew point temperature [oC]
relative_humidity=climate_file(t,3);    %Set relative humidity [%]
solar_intensity=climate_file(t,4);      %Set gloal horiontal radiation intensity [W/m^2]
wind_speed=climate_file(t,5);           %Set wind speed [m/s]
sky_temp=climate_file(t,6);             %Set effective sky temperature [K]
solar_incident_angle=climate_file(t,8);  %Set solar incident angle [o]
atmospheric_pressure=climate_file(t,10);  %Set atmospheric pressure [Pa]
river_temp=climate_file(t,12);          %Set river water temperature [oC]

%%%%%%%%%%%%%%%%%%%%%%%%%%%%%%%%%%%%%%%%%%%%%

Q_fluid_loss=0;         %Set default heat transfer to fluid
Q_heat_abs=limit+1;     %Set default heat transfer to fluid

%Calculate solar radiation heat transfer
solar_incident_rad=solar_incident_angle*pi/180;             %Convert incident angle to radians
refract=asin(sin(solar_incident_rad)*nair/nwater)+0.001;    %Calculate angle of refraction
rperp=(sin(refract-solar_incident_rad))^2/(sin(refract+solar_incident_rad))^2; %Calculate
perpendicular component of reflection
rpara=(tan(refract-solar_incident_rad))^2/(tan(refract+solar_incident_rad))^2;    %Calculate
parallel component of reflection
TAOr=0.5*((1-rperp)/(1+rperp)+(1-rpara)/(1+rpara));     %Calculate transmittance of reservoir
surface
TAOa=exp(-1*extinct*reservoir_depth/cos(refract));     %Calculate absorbance of reservoir surface
reflectivity=TAOa-TAOa*TAOr;                           %Calculate reflectivity of reservoir surface
Q_solar=solar_intensity*(1-reflectivity)*reservoir_area; %Calculate solar radiation heat gain [W]
```

```matlab
%Calculate thermal radiation heat transfer
Q_thermal=reservoir_area*emissivity*(5.67E-8)*((reservoir_temp+273)^4-(sky_temp^4)); %[W]

%Calculate evaporative heat transfer
e0=610.8*exp((17.27*reservoir_temp)/(237.7+reservoir_temp));    %Calculate saturation vapour
pressure [Pa]
ea=610.8*exp((17.27*dew_point)/(237.7+dew_point));%Calculate actual vapour pressure [Pa]
evaprate=0.000968*wind_speed*(e0-ea);              %Calculate water evaporation rate [mm/day]
Q_evap=(2.45*1*evaprate*reservoir_area*1000)/86.4; %Calculate evaporative heat transfer [W

%Calculate sensible heat transfer
Q_sens=Q_evap*66*(dry_bulb-reservoir_temp)/(e0-ea); %[w]

%Calculate energy transfer by addition and removal of water
if river_flow_file(t,1)>0.18
   river_flow_file(t,1)=0.18;
end

if t>2160&&t<7296|t>10920&&t<16056
    river_flow_file(t,1)=0;
  end

Q_water=river_top_up(t,1)*river_flow_file(t,1)*density_water(river_temp)*water_cp(river_temp)*
(river_temp-reservoir_temp); %[W]

%Begin reservoir loop transfer module
if heat_pump_profile(t,1)==1

while abs(Q_fluid_loss-Q_heat_abs)>limit

%Calculate film properties
fluid_average=real((fluid_in+fluid_out)/2);        %Calculate average transfer fluid temperature
[oC]
filmW_T=real((fluid_average+reservoir_temp)/2);    %Calculate film temperature [oC]
C_p=water_cp(filmW_T);                             %Define film specific heat capacity [J/kg.K]
water_dynamic=water_dynamic_viscosity(filmW_T); %Define film dynamic viscosity [kg/m.s]
water_beta=water_expansion(filmW_T);              %Define film thermal expnasion coefficient
[1/K]
water_con=water_conductivity(filmW_T);            %Define film thermal conductivity [W/m.K]
water_density=density_water(filmW_T);             %Define film density [kg/m^3]
water_alpha=water_con/(water_density*C_p);        %Define film thermal diffusivity [m^2/s]
water_kinematic=water_dynamic/water_density;      %Define film kinematic viscosity [m^2/s]

water_Pr=C_p*water_dynamic/water_con;             %Calculate Prandtl number
water_Ra=9.81*water_beta*(reservoir_temp-
fluid_average)*(char_length_x^3)/(water_kinematic*water_alpha);  %Calculate Rayleigh number
```

```
water_Nu=real((0.825+((0.387*water_Ra^(1/6))/(1+(0.492/water_Pr)^(9/16))^(8/27)))^2);
%Calculate Nusselt number
transfer_coeff=water_Nu*water_con/char_length_x;        %Calculate heat transfer coefficient [W]

%Get glycol properties
cp_gly=cp_glycol(fluid_out);
glycol_density=density_water(fluid_average);
mass_flow_rate=(volumetric_flow_rate*glycol_density)/3600;

%Calculate heat transfer
Q_heat_abs=transfer_coeff*exchanger_area*(reservoir_temp-fluid_average);      %Calculate heat
transfer to exchanger
Q_fluid_loss=(mass_flow_rate)*cp_gly*(fluid_out-fluid_in);                    %Calculate heat
gain by fluid

%Perform check for correct outlet temperature
if Q_heat_abs<Q_fluid_loss
fluid_out=fluid_out-temperature_step;
else
fluid_out=fluid_out+temperature_step;
end

end

%Perform heat pump calculations
%Q_pump=1000*(6.4485*fluid_out+134.1);   %Empirical relation 0802 @35
%COP=0.1262*fluid_out+3.8461;            %Empirical relation 0802 @35

%Q_pump=1000*(15.709*fluid_out+334.3);   %Empirical relation 1902 @35
%COP=0.1203*fluid_out+3.8227;            %Empirical relation 1902 @35

Q_pump=1000*(29.092*fluid_out+618.1);    %Empirical relation 3202 @35
COP=0.1266*fluid_out+3.9645;             %Empirical relation 3202 @35

%Q_pump=1000*(6.0486*fluid_out+120.16);  %Empirical relation 0802 @50
%COP=0.0872*fluid_out+2.6803;            %Empirical relation 0802 @50

%Q_pump=1000*(15.014*fluid_out+303.26);  %Empirical relation 1902 @50
%COP=0.0817*fluid_out+2.6543;            %Empirical relation 1902 @50

%Q_pump=1000*(27.223*fluid_out+556.46);  %Empirical relation 3202 @50
%COP=0.0864*fluid_out+2.7764;            %Empirical relation 3202 @50

fluid_in=fluid_out-(Q_pump/(cp_gly*mass_flow_rate));        %Calculate new inlet temperature for
heat exchanger

else
```

```
    Q_fluid_loss=0;
end


%Calculate total energy flow and net energy flow
Q_in=Q_solar+Q_sens+Q_water;              %Calculate heat gain [W]
Q_out=Q_thermal+Q_evap+(1*Q_fluid_loss);  %Calculate heat loss [W]
Q_net=Q_in-Q_out;                         %Calculate net energy transfer [W]

%Define reservoir properties
reservoir_cp=water_cp(reservoir_temp);        %Calculate pond cp
reservoir_rho=density_water(reservoir_temp);  %Calculate pond density

%Calculate temperature change and new reservoir temperature
delta_T=(Q_net*3600)/(reservoir_cp*reservoir_volume*reservoir_rho);   %Calculate delta T for
timestep [K]
reservoir_temp=real(reservoir_temp+delta_T);        %Calculate new reservoir temperature [oC]

%%%%%%%%%%%%%%%%%%%%%%%%%%%%%%%%%%%%%%%%%%%
%Save results to matrix
temperature_results(t,1)=reservoir_temp;
temperature_results(t,2)=Q_pump;
temperature_results(t,3)=COP;
temperature_results(t,4)=filmW_T;
temperature_results(t,4)=fluid_average;
temperature_results(t,5)=fluid_in;
temperature_results(t,6)=fluid_out;

energy_results(t,1)=Q_solar;
energy_results(t,2)=Q_sens;
energy_results(t,3)=Q_thermal;
energy_results(t,4)=Q_evap;
energy_results(t,5)=Q_fluid_loss;
energy_results(t,6)=Q_heat_abs;
energy_results(t,7)=Q_pump;

%Set time for next timestep
t=t+1;
end

%%%%%%%%%%%%%%%%%%%%%%%%%%%%%%%%%%%%%%%%%%%
%Save model results to .csv file
plot(temperature_results(:,1))                   %Plot temperature of reservoir
xlim([tstart,tend])
csvwrite('main_results.csv',temperature_results) %Write main results to .csv file
csvwrite('energy_results.csv',energy_results)    %Write enegy transfer results to .csv file
```

6.3 Material property relations

Properties of water and glycol solution were calculated according to the relations given here.

6.3.1 Water

Density

bg0=999.83952;
bg1=16.945176;
bg2=-0.0079870401;
bg6=0.01687985;
bg3=-46.170461E-06;
bg4=105.56302E-09;
bg5=-280.54253E-12;
waterdensity=(bg0+T*(bg1+T*(bg2+T*(bg3+T*(bg4+T*bg5)))))/(1+bg6*T);

Specific heat capacity

ACP0=4.21534;
ACP1=-0.00287819;
ACP2=7.4729E-05;
ACP3=-7.79624E-07;
ACP4=3.220424E-09;
WCP=ACP0+T*(ACP1+T*(ACP2+T*(ACP3+T*ACP4)));
waterspecificheat=WCP*1000;

Dynamic viscosity

am0=-3.30233;
am1=1301;
am2=998.333;
am3=8.1855;
am4=0.00585;
am5=1.002;
am6=-1.3272;
am7=-0.001053;
am8=105;
am10=0.68714;
am11=-0.0059231;
am12=2.1249E-5;
am13=-2.69575E-8;
wmu=am5*10^((T-20)*(am6+(T-20)*am7)/(T+am8));
if T<20
wmu=10^(am0+am1/(am2+(T-20)*(am3+am4*(T-20))))*100;

```
end
dynamic_viscosity=0.001*wmu;
```

Expansion coefficient

```
expansion=1.060228571E-5*T+3.956E-5;
```

Conductivity

```
ak0=0.560101;
ak1=0.00211703;
ak2=-1.05172E-5;
ak3=1.497323E-8;
ak4=-1.48553E-11;
conductivity=ak0+T*(ak1+T*(ak2+T*(ak3+T*ak4)));
```

6.3.2 Glycol

Specific heat capacity

```
afspecificheat=4186.6*(0.89889+((5.1554E-4)*T));
```

7 References

Alliant Energy (2013), *Case Studies: Great River Medical Center.* [online] Available at:

http://www.alliantenergy.com/SaveEnergyAndMoney/RenewableEnergy/Geothermal/ 030618. [Accessed 13 June 2013]

American Society of Heating, Refrigeration and Air-Conditioning (ASHRAE) (2009), *2009 ASHRAE Handbook.* Atlanta, GA: ASHRAE

AWEB Supply (2013), *Slim Jim Geo Lake Plate* [online] Available at: http://www.awebgeo.com/slim_jim_geo_lake_plate_home.html. [Accessed 13 June 2013].

AWEB Supply (2013), *Slim Jim® Geo Lake Plate® Comparison* [online] Available at: http://www.awebgeo.com/comparison.html. [Accessed 13 June 2013].

Banks, D. (2012), *An Introduction to Thermogeology: Ground Source Heating and Cooling.* 2nd ed. Oxford: Wiley-Blackwell.

Bliss, R. W. Jr. (1961) Atmospheric Radiation Near the Surface of the Ground: A Summary for Engineers. *Solar Energy.* 5 (3): 103-120.

Carbon Trust (2010), How to implement guide on ground source heat pumps. [online] Available at:

http://www.carbontrust.com/media/147462/j8057_ctl150_how_to_implement_guide_ on_ground_source_heat_pumps_aw__interactive.pdf

Chiasson, A. D., Spitler, J. D., Rees, S. J., Smith, M. D. (2000), A Model for Simulating the Performance of a Shallow Pond as a Supplemental Heat Rejecter with Closed-Loop Ground-Source Heat Pump Systems. *ASHRAE Transactions.* 106: 107-121.

Chua, K. J., Chou, S. K., Yang, W. M. (2010), Advances in heat pump systems: A review. *Applied Energy*, 87: 3611-3624.

Climaveneta, (2013). *Commercial and industrial heat pumps: RECS-W 0802-3202* [online] Available at: http://www.climaveneta.com/GLOBAL/Products/17/commercial-and-industrial-heat-pumps/water-cooled-reversible-heat-pumps/73/recs-w-0802-3202.html

DC Thomson & Co., Ltd, (2013). *St Andrews University considers renewable energy project for former Guardbridge paper mill* [online] Available at: http://www.thecourier.co.uk/news/local/fife/st-andrews-university-considers-renewable-energy-project-for-former-guardbridge-paper-mill-1.39714 [Accessed 12 July 2013].

Duffie, J. A., Beckman, W. A. (1991) *Solar engineering of thermal processes*. New York: Wiley.

Egg, J., Howard, B. C. (2011), *Geothermal HVAC: Green heating and cooling*. New York: McGraw-Hill.

The Energy Savings Trust (2004), Domestic Ground Source Heat Pumps: Design and installation of closed-loop systems. [online] Available at: http://www.gshp.org.uk/documents/ce82-domesticgroundsourceheatpumps.pdf

The Energy Savings Trust (2010), Getting warmer: a field trial of heat pumps. [online] Available at: http://www.heatpumps.org.uk/PdfFiles/TheEnergySavingTrust-GettingWarmerAFieldTrialOfHeatPumps.pdf.

The Engineering Toolbox (2013), *Ethylene Glycol Heat-Transfer Fluid*. [online] Available at: http://www.engineeringtoolbox.com/ethylene-glycol-d_146.html [Accessed 24 Aug 2013]

European Committee for Standardization (ECS) (2007), Air conditioners, liquid chilling packages and heat pumps with electrically driven compressors for space heating and cooling – Part 3: Test methods. [online] Available at: http://www.energy.ca.gov/title24/2008standards/special_case_appliance/altherma_heat_pump/Daikin_Altherma_CompOpApplication/Referenced%20European%20Standards/EN%2014511-3%20(2007).pdf.

Freemat (2013), *Freemat homepage*. [online] Available at: http://freemat.sourceforge.net/#home [Accessed 19 August 2013]

Google Earth 7.1, (2013). *Guardbridge mill loch reservoir 56°22'07.66"N, 2°53'44.44"W, elevation 7M. Available through: http://www.google.com/earth/index/html [Accessed 24 July 2023]*

The Green Blue (2013), Installing Heat Pumps to Reduce Energy Consumption. [online] Available at: http://www.thegreenblue.org.uk/pdf/Case%20Study%2013%20Installing%20Heat%20Pumps%20British%20Waterways.pdf

Halcrow Group Ltd., (2013). *Reservoirs Act 1975 Supervising Engineer's Inspection*. [hardcopy]

Hayes, T., Song, L., Dawson, M., Chancellor, A. (2012), Heat Balance Analysis to Validate the Heat Dissipation Rate of a Man-Made Lake as a Heat Rejection Device in a Power Plant. *International Journal of Renewable Energy Research.* 2 (1): 78-83.

Hostetler, S. W. (1995) Hydrological and thermal response of lakes to climate change: Description and modelling. In: Lerman, A. Imboden, D. M., Gat, J. R. (eds.), *Physics and Chemistry of Lakes*, 2nd ed. Berlin: Springer-Verlag, pp.63-82.

Hsieh, J. S. (1986), *Solar energy engineering*. New Jersey: Prentice-Hall.

Hull, J.R., Liu, K.V., Sha, W.T., Kamal, J., Nielsen, C.E. (1984), Dependence of ground heat losses upon solar pond size and perimeter insulation - Calculated and experimental results. *Solar Energy* 33(1): 25-33.

Incropera, F. P., DeWitt, D. P., Bergman, T. L., Lavine, A. S. (2007) *Fundamentals of heat and mass transfer*, 6th ed. Hoboken, NJ:John Wiley.

International Energy Agency (IEA) Heat Pump Centre, *Heat pump performance.* [online] Available at: http://www.heatpumpcentre.org/en/aboutheatpumps/heatpumpperformance/Sidor/default.aspx [Accessed 13 June 2013]

Irvine, T. F., Liley, P. E. (1984) *Steam and Gas Tables with Computer Equations.* United States: Academic Press.

Karpathy, Z. (2012), Heat Pump Markets: UK in Europe. [online] Available at: http://www.heatpumpcentre.org/en/hppactivities/hppworkshops/London2012/Documents/02_Z_Karpathy.pdf.

KJWW Engineering Consultants (2013), *Project Details.* [online] http://www.kjww.com/ProjectDetails.aspx?ProjectNumber=C9.6071.00 [Accessed 12 July 2013]

Laval, B. (2006), *Civil 542, Physical limnology, 2.0D budgets.* Course notes (2006), Department of Civil Engineering, University of British Columbia, Canada.

Linacre, E. (1992), *Climate and Data Resources: A Reference and Guide.* London: Routledge, pp365.

MEGlobal, (2008) Ethylene Glycol Product Guide [online] Available at: http://www.meglobal.biz/media/product_guides/MEGlobal_MEG.pdf.

Mountain Empire Community College, (n.d.). [image online] Available at: http://water.me.vccs.edu/courses/ENV115/clipart/baylis.gif [Accessed 8 Sep 2013]

National Environment Research Council, Centre for Ecology & Hydrology (2013) *National River Flow Archive Data, Motray Water at St Michaels*. [online] Available at: http://www.ceh.ac.uk/data/nrfa/data/time_series.html?14005 [Accessed 23 Aug 2013]

Omer, A. M. (2008), Ground-source heat pumps systems and applications. *Renewable and Sustainable Energy Reviews*. 12: 344-371.

Ordnance Survey, (2012). *Guardbridge overview,* 1:2000, 1:300. OSgetamap [online] Available through: http://www.getamap.ordnancesurveyleisure.co.uk/ [Accessed 12 July 2013].

The Parliamentary Office of Science & Technology. (2013), Residential Heat Pumps. [online] Available at: http://www.parliament.uk/briefing-papers/POST-PN-426.

Pezant, M. C., Kevanaugh, S. P. (1990), Development and verification of a thermal model of lakes used with water source heat pumps." *ASHRAE Transactions*. 96 (1): 574-582.

Phillips, N. (2013), *New Lanark WSHP*. [email] (Personal communication, 1 August 2013).

Renew-Reuse-Recycle (2009), *Innovative technology at Kings Mill Hospital cuts carbon footprint and saves thousands of pounds a year*. [online] Available at: http://www.renew-reuse-recycle.com/showarticle.pl?id=1452. [Accessed 10 June 2013]

R & M Wheildon Limited (2012), *Lake House Hotel Utilises Solar and Ground Source Heating*. [online] Available at: http://www.wheildons.co.uk/lake-house-hotel-solar-and-ground-source-heating/. [Accessed 13 June 2013]

Scottish Environment Protection Agency (SEPA) (2013), *EC Reporting Directive.* [email] (Personal communication, 6 August 2013).

The Scottish Government (undated), Tall Ship Water Source Heat Pump. [online] Available   at: http://www.communityenergyscotland.org.uk/assets/0001/0924/Tall_Ship_-_P40462.pdf.

The Scottish Government (2012), *National indicators (2007), Electricity*. [online] Available   at: http://www.scotland.gov.uk/About/Performance/scotPerforms/indicators/electricity [Accessed 25 Aug 2013]

Stiebel Eltron, *The wonders of watersource.* [online] Available at: http://www.stiebel-eltron.co.uk/business-partners/news/technical-expert-blog/the-wonders-of-water-source/. [Accessed 13 June 2013]

Stoke-on-Trent City Council (2013a), *Westport Lake*. [online] Available at: http://www.stoke.gov.uk/ccm/content/leisure-and-culture/parks-and-open-spaces/westport-lake.en;jsessionid=aUAndsdRIZp6. [Accessed 13 June 2013]

Stoke-on-Trent City Council (2013b), *Westport Lake Visitors Centre.* [online] Available   at: http://www.stoke.gov.uk/ccm/content/environment/climate-change/climate-change-case-studies.en.

Sumner, J. A. (1948) The Norwich Heat Pump. *Proceedings of the Institution of Mechanical Engineers.* 158: 22-29.

UFW Limited (2013), Waterton Park Hotel (Case study). Available at: http://www.ufw.co.uk/products-technologies/heat-pumps/ground-source-heat-pumps/#tabs

University of St Andrews, (2004). *Reservoir Act 1975 Prescribed from of record for a large raised reservoir.* [hardcopy]

YouGen (2012), *An introduction to water source heat pumps and how they work.* [online] Available at: http://www.yougen.co.uk/blog-entry/1954/An+introduction+to+water+source+heat+pumps+and+how+they+work/ [Accessed 17 Aug 2013]

Yarr, R. (2013), [phone conversation] (Personal communication, June 2013).

Young, J. (2013), *RECS-W heat pump performance*. [email] (Personal communication, 26 August 2013).